

1 **Plant responses to volcanically-elevated CO<sub>2</sub> in two Costa Rican**  
2 **forests**

3 Robert R. Bogue<sup>1,2</sup>, Florian M. Schwandner<sup>1,3</sup>, Joshua B. Fisher<sup>1</sup>, Ryan Pavlick<sup>1</sup>, Troy S. Magney<sup>1</sup>,  
4 Caroline A. Famiglietti<sup>1</sup>, Kerry Cawse-Nicholson<sup>1</sup>, Vineet Yadav<sup>1</sup>, Justin P. Linick<sup>1</sup>, Gretchen B.  
5 North<sup>4</sup>, Eliecer Duarte<sup>5</sup>

6 <sup>1</sup>Jet Propulsion Laboratory, 4800 Oak Grove Drive, Pasadena, CA 91109, USA

7 <sup>2</sup>Geology Department, Occidental College, 1600 Campus Road, Los Angeles, CA 90041, USA

8 <sup>3</sup>Joint Institute for Regional Earth System Science and Engineering, University of California Los Angeles, Los  
9 Angeles, CA 90095

10 <sup>4</sup>Biology Department, Occidental College, 1600 Campus Road, Los Angeles, CA 90041, USA

11 <sup>5</sup>Observatory of Volcanology and Seismology (OVSICORI), Universidad Nacional de Costa Rica, 2386-3000  
12 Heredia, Costa Rica

13 Correspondence to: Florian.Schwandner@jpl.nasa.gov

14

15

16

Revised manuscript prepared for:

17

Biogeosciences (Copernicus), <https://www.biogeosciences.net/>

18

REV1 (2018-07-19)

19

20 **Abstract.** We explore the use of active volcanoes to determine the short- and long-term effects of elevated CO<sub>2</sub> on  
21 tropical trees. Active volcanoes continuously but variably emit CO<sub>2</sub> through diffuse emissions on their flanks,  
22 exposing the overlying ecosystems to elevated levels of atmospheric CO<sub>2</sub>. We found tight correlations ( $r^2=0.86$  and  
23  $r^2=0.74$ ) between wood stable carbon isotopic composition and co-located volcanogenic CO<sub>2</sub> emissions for two  
24 species, which documents the long-term photosynthetic incorporation of isotopically heavy volcanogenic carbon into  
25 wood biomass. Measurements of leaf fluorescence and chlorophyll concentration suggest that volcanic CO<sub>2</sub> also has  
26 measurable short-term functional impacts on select species of tropical trees. Our findings indicate significant potential  
27 for future studies to utilize ecosystems located on active volcanoes as natural experiments to examine the ecological  
28 impacts of elevated atmospheric CO<sub>2</sub> in the tropics and elsewhere. Results also point the way toward a possible future  
29 utilization of ecosystems exposed to volcanically elevated CO<sub>2</sub> to detect changes in deep volcanic degassing by using  
30 selected species of trees as sensors.

## 31 **1 Introduction**

32 Tropical forests represent about 40% of terrestrial Net Primary Productivity (NPP) worldwide, store 25% of biomass  
33 carbon, and may contain 50% of all species on Earth, but the projected future responses of tropical plants to globally  
34 rising levels of CO<sub>2</sub> are poorly understood (Leigh et al., 2004; Townsend et al., 2011). The largest source of uncertainty  
35 comes from a lack of understanding of long-term CO<sub>2</sub> fertilization effects in the tropics (Cox et al., 2013). Reducing  
36 this uncertainty would significantly improve Earth system models, advances in which would help better constrain  
37 projections in future climate models (Cox et al., 2013; Friedlingstein et al., 2013). Ongoing debate surrounds the  
38 question of how much more atmospheric CO<sub>2</sub> tropical ecosystems can absorb—the “CO<sub>2</sub> fertilization effect” (Gregory  
39 et al., 2009; Kauwe et al., 2016; Keeling, 1973; Schimel et al., 2015).

40 Free Air CO<sub>2</sub> Enrichment (FACE) experiments have been conducted to probe this question, but none have  
41 been conducted in tropical ecosystems (e.g. Ainsworth and Long, 2005; Norby et al., 2016). Some studies have used  
42 CO<sub>2</sub>-emitting natural springs to study plant responses to elevated CO<sub>2</sub>, but these have been limited in scope due to the  
43 small spatial areas around springs that experience elevated CO<sub>2</sub> (Paoletti et al., 2007; Saurer et al., 2003). These studies  
44 have suffered from several confounding influences, including other gas species that accompany CO<sub>2</sub> emissions at  
45 these springs, human disturbances, and difficulty with finding appropriate control locations. Additionally, none have  
46 been conducted in the tropics (Pinkard et al., 2010). A series of studies in Yellowstone National Park (USA) used its  
47 widespread volcanic hydrothermal CO<sub>2</sub> emissions for the same purpose, though it is not in the tropics (Sharma and  
48 Williams, 2009; Tercek et al., 2008). Yellowstone was particularly suitable for this type of study, due to its protected  
49 status as a National Park, and because the large areas of CO<sub>2</sub> emissions made control points more available (Sharma  
50 and Williams, 2009; Tercek et al., 2008). These studies reported changes in rubisco, an enzyme central to CO<sub>2</sub> fixation,  
51 and sugar production in leaves similar to results from FACE experiments, suggesting that volcanically-influenced  
52 areas like Yellowstone have untapped potential for studying the long-term effects of elevated CO<sub>2</sub> on plants.

53 Tropical ecosystems on the vegetated flanks of active volcanoes offer large and diverse ecosystems that could  
54 make this type of study viable. Well over 200 active volcanoes are in the tropics (Global Volcanism Program, 2013)  
55 and many of these volcanoes are heavily forested. However, fewer of these tropical volcanic forests have sufficient

56 legal protection to be a source of long-term information, and the effects of diffuse volcanic flank gas emissions on the  
57 overlying ecosystems remain largely unknown. Most previous studies focused on extreme conditions, such as tree kill  
58 areas associated with extraordinarily high CO<sub>2</sub> emissions at Mammoth Mountain, CA (USA) (Biondi and Fessenden,  
59 1999; Farrar et al., 1995; Sorey et al., 1998). However, the non-lethal effects of volcanic CO<sub>2</sub>—away from the peak  
60 emission zones, but still in the theorized fertilization window—have received little attention, and could offer a new  
61 approach to studying the effects of elevated CO<sub>2</sub> on ecosystems (Cawse-Nicholson et al., 2018). The broad flanks of  
62 active volcanoes experience diffuse emissions of excess CO<sub>2</sub> because the underlying active magma bodies  
63 continuously release gas, dominated by CO<sub>2</sub> transported to the surface along fault lines (Chiodini et al., 1998; Dietrich  
64 et al., 2016; Farrar et al., 1995). This process has frequently been studied to understand the dynamics of active magma  
65 chambers and to assess potential volcanic hazards (Chiodini et al., 1998; Sorey et al., 1998). These emissions are  
66 released through faults and fractures on the flanks of the volcano (Burton et al., 2013; Pérez et al., 2011; Williams-  
67 Jones et al., 2000)(see Supplementary Figure S1). Volcanic flanks through which these gases emanate are broad,  
68 covering typically 50-200 km<sup>2</sup>, often supporting well-developed, healthy ecosystems. Some of these faults tap into  
69 shallow acid hydrothermal aquifers, but by the time these gases reach the surface of most forested volcanoes, soluble  
70 and reactive volcanic gas species (e.g., SO<sub>2</sub>, HF, HCl, H<sub>2</sub>S) have been scrubbed out in the deep subsurface, leading to  
71 a diffusely emanated gas mix of predominantly CO<sub>2</sub> with minor amounts of hydrogen, helium, and water vapor  
72 reaching the surface (Symonds et al., 2001).

73 Trees in these locations are continuously exposed to somewhat variably elevated levels of CO<sub>2</sub> (eCO<sub>2</sub>),  
74 though it is unclear if the trees utilize this excess CO<sub>2</sub>. Volcanic CO<sub>2</sub> has a heavy δ<sup>13</sup>C signature typically ranging  
75 from -7 to -1 ‰, which is distinct from typical vegetation and noticeably heavier than typical atmospheric values  
76 (Mason et al., 2017). If trees incorporate volcanic CO<sub>2</sub>, then the stable carbon isotopic composition of wood may  
77 document the long-term, possibly variable influence of volcanic CO<sub>2</sub> during the tree's growth. With this tracer  
78 available, volcanic ecosystems could become a valuable natural laboratory to study the long-term effects of elevated  
79 CO<sub>2</sub> on ecosystems, especially in understudied regions like the tropics. Additionally, short-term effects of eCO<sub>2</sub> might  
80 be revealed by plant functional measurements at the leaf scale, where the additional CO<sub>2</sub> could increase carbon uptake  
81 in photosynthesis.

82 Here we provide preliminary results on the short- and long-term non-lethal impacts of diffuse volcanic CO<sub>2</sub>  
83 emissions on three species of tropical trees on the flanks of two active volcanoes in Costa Rica. We also explore the  
84 viability of studying volcanically-influenced ecosystems to better understand potential future responses to elevated  
85 CO<sub>2</sub>, and suggest adjustments to our approach that will benefit future, similarly-motivated studies.

## 86 **2 Methods**

### 87 **2.1 Investigated locations and sampling strategy**

88 Irazú and Turrialba are two active volcanoes located ~25 and 35 km east of San José, Costa Rica (Fig. 1). These two  
89 volcanoes are divided by a large erosional basin. The two volcanoes cover approximately 315 km<sup>2</sup>, which is  
90 significantly larger than the average forested active volcanic edifice in Costa Rica at 122 km<sup>2</sup>. The vast majority of

91 the northern flanks of Irazú and Turrialba are covered in legally protected dense old-growth forest, while the southern  
92 flanks are dominated by pasture land and agriculture. Turrialba rises 3,300 m above its base and has been active for  
93 at least 75,000 years with mostly fumarolic activity since its last major eruption in 1866 (Alvarado et al., 2006). It has  
94 experienced renewed activity beginning in 2010, and its current activity is primarily characterized by a near-constant  
95 volcanic degassing plume, episodic minor ash emissions, and fumarolic discharges at two of the summit craters, as  
96 well as significant diffuse and fumarolic gas emissions across its flanks, focused along fault systems (Martini et al.,  
97 2010). Turrialba's CO<sub>2</sub> emissions in areas proximal to the crater were calculated at 113 ± 46 tons/d (Epiard et al.,  
98 2017). The Falla Ariete (Ariete fault), a major regional fault, runs northeast-southwest through the southern part of  
99 Turrialba's central edifice and is one of the largest areas of diffuse CO<sub>2</sub> emissions on Turrialba (Epiard et al., 2017;  
100 Rizzo et al., 2016). Atmospheric CO<sub>2</sub> has an average δ<sup>13</sup>C value of -9.2 ‰ at Turrialba, and the volcanic CO<sub>2</sub> released  
101 at the Ariete fault has significantly heavier δ<sup>13</sup>C values clustered around -3.4 ‰ (Malowany et al., 2017).

102 Irazú has been active for at least 3,000 years, and had minor phreato-magmatic eruptions in 1963 and a single  
103 hydrothermal eruption in 1994. Currently, Irazú's activity primarily consists of shallow seismic swarms, fumarolic  
104 crater gas emissions, small volcanic landslides, and minor gas emissions on its northern forested flank (Alvarado et  
105 al., 2006; Barquero et al., 1995). Diffuse cold flank emissions of volcanic CO<sub>2</sub> represent the vast majority of gas  
106 discharge from Irazú, as the main crater releases 3.8 t d<sup>-1</sup> of CO<sub>2</sub> and a small area on the north flank alone releases 15  
107 t d<sup>-1</sup> (Epiard et al., 2017). Between the two volcanoes, a major erosional depression is partially occupied by extensive  
108 dairy farms, and is somewhat less forested than their flanks.

109 In this study, we focused on accessible areas between 2,000 and 3,300 m on both volcanoes (Fig. 1). On  
110 Irazú, we sampled trees and CO<sub>2</sub> fluxes from the summit area to the north, near the approximately north-south striking  
111 Rio Sucio fault, crossing into the area dominated by dairy farms on Irazú's lower NE slope. Our sampling locations  
112 on Irazú were located along a road from the summit northward down into this low-lying area. On Turrialba, we focused  
113 on an area of known strong emissions but intact forests on the SW slope, uphill of the same erosional depression, but  
114 cross-cut by the major NE-SW trending active fracture system of the Falla Ariete. We sampled three main areas of  
115 the Falla Ariete, each approximately perpendicularly transecting the degassing fault along equal altitude; the upper  
116 Ariete fault, the lower Ariete fault, and a small basin directly east of the old Cerro Armado cinder cone on Turrialba's  
117 south-western flank. We took a total of 51 tree samples (17 were excluded after stress screening) at irregular intervals  
118 depending on the continued availability and specimen maturity of three species present throughout the transect.

119 All transects are in areas experiencing measurable CO<sub>2</sub> enhancements from the Falla Ariete, but not high  
120 enough to be in areas generally downwind of the prevailing crater emissions plume (Epiard et al., 2017). We avoided  
121 areas that experience ash fall, high volcanic SO<sub>2</sub> concentrations, local anthropogenic CO<sub>2</sub> from farms, or that were  
122 likely to have heavily acidified soil. Excessively high soil CO<sub>2</sub> concentrations can acidify soil, leading to negative  
123 impacts on ecosystems growing there (McGee and Gerlach, 1998). Because such effects reflect by-products of extreme  
124 soil CO<sub>2</sub> concentrations rather than direct consequences of elevated CO<sub>2</sub> on plants, we avoided areas with CO<sub>2</sub> fluxes  
125 high enough to possibly cause noticeable CO<sub>2</sub>-induced soil acidification. Light ash fall on some days likely derived  
126 from atmospheric drift, as we were not sampling in areas downwind of the crater. The ash fall did not in any noticeably  
127 way affect our samples, as trees showing ash accumulation on their leaves or previous damage were the exception and

128 avoided. Altitude, amount of sunlight during measurements, and aspect had no consistent correlations with any of the  
129 parameters we measured.

## 130 **2.2 Studied tree species**

131 Our study focused on three tree species found commonly on Turrialba and Irazú: *Buddleja nitida*, *Alnus acuminata*,  
132 and *Oreopanax xalapensis*. *Buddleja nitida* is a small tree with a typical stem diameter (DBH) ranging from 5 to 40  
133 cm that grows at elevations of 2,000-4,000 m throughout most of Central America (Kappelle et al., 1996; Norman,  
134 2000). The DBH of the individuals we measured ranged from 11.5 to 51.3 cm, with an average of 29.85 cm. It averages  
135 4-15 m in height and grows primarily in early and late secondary forests (Kappelle et al., 1996; Norman, 2000). *Alnus*.  
136 *acuminata* is a nitrogen-fixing pioneer species exotic to the tropics that can survive at elevations from 1,500-3,400 m,  
137 although it is most commonly found between 2,000-2,800 m (Weng et al., 2004). The trees we measured had DBH  
138 ranging from 14.3 to 112 cm, with an average of 57.14 cm. *Oreopanax xalapensis* thrives in early and late successional  
139 forests, although it can survive in primary forests as well (Kappelle et al., 1996; Quintana-Ascencio et al., 2004). It  
140 had the smallest average DBH of the three species, ranging from 6.6 to 40.9 cm, with an average of 22.71 cm.

## 141 **2.3 CO<sub>2</sub> concentrations and soil diffuse flux measurements**

142 Soil CO<sub>2</sub> flux was measured with an accumulation chamber near the base of the tree (generally within 5 meters, terrain  
143 permitting) at three different points and then averaged to provide a single CO<sub>2</sub> flux value to compare to the <sup>13</sup>C  
144 measurement of the corresponding tree sample. This technique is intended to provide a simple relative way to compare  
145 the CO<sub>2</sub> exposure of different trees, as a tree with high CO<sub>2</sub> flux near its base should experience consistently higher  
146 CO<sub>2</sub> concentrations than a tree with lower CO<sub>2</sub> flux. We also measured concentrations at ground level and 1.5 – 2.0  
147 m above ground level, though these were expectedly highly variable in time and location. We used a custom-built soil  
148 flux chamber system which contained a LI-COR 840A non-dispersive infrared CO<sub>2</sub> sensor (LI-COR Inc., Lincoln NE,  
149 USA) to measure soil CO<sub>2</sub> flux. A custom-built cylindrical accumulation chamber of defined volume was sealed to  
150 the ground and remained connected to the LI-COR sensor. The air within the accumulation chamber was continuously  
151 recirculated through the sensor, passing through a particle filter. The sensor was calibrated before deployment and  
152 performed within specifications. We recorded cell pressure and temperature, ambient pressure, air temperature, GPS  
153 location, time stamps, location description, soil type and cover, wind speed and direction, relative humidity, and slope,  
154 aspect, and altitude as ancillary data. In typical operation, each measurement site for flux measurements was validated  
155 for leaks (visible in the live data stream display as spikes and breaks in the CO<sub>2</sub> concentration slope), and potential  
156 external disturbances were avoided (such as vehicle traffic, generators, or breathing animals and humans).  
157 Measurements were recorded in triplicate for at least 2 minutes per site. Data reduction was performed using recorded  
158 time stamps in the dataset, with conservative time margins to account for sensor response dead time, validated against  
159 consistent slope sections of increasing chamber CO<sub>2</sub>. Fluxes were computed using ancillary pressure and temperature  
160 measurements and the geometric chamber constant (chamber volume at inserted depth, tubing volume, and sensor  
161 volume). Care was taken to not disturb the soil and overlying litter inside and adjacent to, the chamber.

## 162 **2.4 Leaf function measurements**

163 Chlorophyll fluorescence measurements were conducted on leaves of all three species during the field campaign to  
164 obtain information on instantaneous plant stress using an OS30p+ fluorometer (Opti-Sciences Inc., Hudson, NH,  
165 USA). Five mature leaves from each individual tree were dark adapted for at least 20 minutes to ensure complete  
166 relaxation of the photosystems. After dark adaptation, initial minimal fluorescence was recorded ( $F_0$ ) under conditions  
167 where we assume that photosystem II (PSII) was fully reduced. Immediately following the  $F_0$  measurement, a 6,000  
168  $\mu\text{mol m}^{-2} \text{s}^{-1}$  saturation pulse was delivered from an array of red LEDs at 660 nm to record maximal fluorescence  
169 emission ( $F_m$ ), when the reaction centers are assumed to be fully closed. From this, the variable fluorescence was  
170 determined as  $F_v/F_m = (F_m - F_0)/F_m$ .  $F_v/F_m$  is a widely used chlorophyll fluorescence variable used to assess the  
171 efficiency of PSII and, indirectly, plant stress (Baker and Oxborough, 2004). The five  $F_v/F_m$  measurements were  
172 averaged to provide a representative value for each individual tree. Some trees had less than five measurements due  
173 to the dark adaptation clips slipping off the leaf before measurements could be taken. Ten trees had four measurements,  
174 and another six had three measurements

175 Chlorophyll concentration index (CCI) was measured with a MC-100 Apogee Instruments chlorophyll  
176 concentration meter (Apogee Instruments, Inc., Logan, UT, USA). CCI was converted to chlorophyll concentration  
177 ( $\mu\text{mol m}^{-2}$ ) with the generic formula derived by Parry et al., 2014. Depending on availability, between three and six  
178 leaves were measured for CCI for each tree, and then averaged to provide a single value for each tree. If leaves were  
179 not within reach, a branch was pulled down or individual leaves were shot down with a slingshot and collected.  
180 Photosynthetically active radiation was measured at each tree with a handheld quantum meter (Apogee Instruments,  
181 Logan, UT, USA) (Table S2). Stomatal conductance to water vapor,  $g_s$  ( $\text{mmol m}^{-2} \text{s}^{-1}$ ) was measured between 10:00-  
182 14:00 hours using a steady-state porometer (SC-1, Decagon Devices, Inc., Pullman, WA, USA), calibrated before use  
183 and read in manual mode. This leaf porometer was rated for humidity <90%, and humidity was sometimes above this  
184 limit during our field work. Consequently, we have fewer stomatal conductance measurements than our other data  
185 types.

## 186 **2.5 Isotopic analysis**

187 We collected wood cores from 31 individual trees at a 1.5 m height using a 5.15 mm diameter increment borer (JIM  
188 GEM, Forestry Suppliers Inc., Jackson, MS, USA). Since no definable tree rings were apparent, we created a fine  
189 powder for isotope analysis by drilling holes into dried cores using a dry ceramic drill bit (Dremel) along the outermost  
190 5 cm of wood below the bark, which was chosen to represent the most recent carbon signal for  $^{13}\text{C}$  analyses. The fine  
191 powder (200 mesh, 0.2 – 5 mg) was then mixed and a random sample was used to extract  $^{13}\text{C}/^{12}\text{C}$  ratios (to obtain  
192  $\delta^{13}\text{C}$  values against the VPDB standard), which we estimated to be representative of at least the last 2-3 years, based  
193 on analogous literature growth rate values: *Oreopanax xalapensis* and *Alnus acuminata* range from 0.25 - 2.5 cm/y  
194 and 0.6 - 0.9 cm/y, respectively (Kappelle et al., 1996; Ortega-Pieck et al, 2011). These rates result in a 5 cm range of  
195 at least 2 and 5.5 years, though the high rates were determined for very young trees under very different conditions  
196 and it is explicitly unknown in our study. Since we only sample the most recent years, no isotopic discrimination  
197 against atmospheric  $^{13}\text{C}$  due to preferential diffusion and carboxylation of  $^{12}\text{C}$ , was conducted. Rather, we assume that

198  $\delta^{13}\text{C}$  values are representative of the relative amount of volcanic  $\text{CO}_2$  vs. atmospheric  $\text{CO}_2$  sequestered by the tree  
199 over the period of growth represented in the sample.  $\delta^{13}\text{C}$  values were determined by continuous flow dual isotope  
200 analysis using a CHNOS Elemental Analyzer and IsoPrime 100 mass spectrometer at the University of California  
201 Berkeley Center for Stable Isotope Biogeochemistry. External precision for C isotope determinations is  $\pm 0.10\%$ . Ten  
202  $\delta^{13}\text{C}$  measurements did not have corresponding soil  $\text{CO}_2$  flux measurements due to the flux measurements being  
203 unavailable for the final two days of sampling, and another 5 samples were from trees that showed signs of extreme  
204 stress, such as browning leaves or anomalously low fluorescence measurements. Since the purpose of our study was  
205 to explore the non-lethal effects of volcanic  $\text{CO}_2$  on trees, during analysis we excluded all trees that were observed in  
206 the field to show visible signs of stress, or that were not fully mature. After these exclusions, all remaining tree cores  
207 with co-located  $\text{CO}_2$  flux measurements were from Turrialba.

208

## 209 **2.6 Sulfur dioxide probability from satellite data**

210 To assess the likelihood of trees having been significantly stressed in the past by volcanic sulfur dioxide ( $\text{SO}_2$ ) from  
211 the central crater vents, we took two approaches. First, we were guided by in-situ measurements taken in the same  
212 areas by Jenkins et al. (2012), who assessed the physiological interactions of  $\text{SO}_2$  and  $\text{CO}_2$  on vegetation on the uppers  
213 lobes of Turrialba and demonstrated a rapid exponential decay of  $\text{SO}_2$  away from the central vent. Second, for long-  
214 term exposure we derived the likelihood of exposure per unit area using satellite data sensitive to  $\text{SO}_2$  (Fig. 2). The  
215 Advanced Spaceborne Thermal Emission and Reflection Radiometer (ASTER), launched in December 1999 on  
216 NASA's Terra satellite, has bands sensitive to  $\text{SO}_2$  emission in the thermal infrared (TIR), at  $\sim 60\text{ m} \times 60\text{ m}$  spatial  
217 resolution. We initially used ASTER Surface Radiance TIR data (AST\_09T), using all ASTER observations of the  
218 target area over the entirety of the ASTER mission (October 2000 until writing in late 2017). The TIR bands were  
219 corrected for downwelling sky irradiance and converted into units of  $\text{W m}^{-2} \mu\text{m}^{-1}$ . For each observation, an absorption  
220 product is calculated by subtracting  $\text{SO}_2$ -insensitive from  $\text{SO}_2$ -sensitive bands:

$$221 \quad S^t = (b_{10} + b_{12}) - 2 \cdot b_{11} \quad (1)$$

222 Where  $S$  is the  $\text{SO}_2$  index,  $t$  is an index representing the time of acquisition,  $b_{10}$  is the radiance at band 10 (8.125 -  
223 8.475  $\mu\text{m}$ ),  $b_{11}$  is the radiance at band 11 (8.475 - 8.825  $\mu\text{m}$ ), and  $b_{12}$  is the radiance at band 12 (8.925 - 9.275  $\mu\text{m}$ ).  
224 This is similar to the method of Campion et al., 2010. The granules were then separated into day and night scenes,  
225 projected onto a common grid, and then thresholded to  $S > 0.1\text{ W m}^{-2} \mu\text{m}^{-1}$ , and converted into a probability. The  
226 output is a spatial dataset that describes the probability of an ASTER observation showing an absorption feature above  
227 a  $0.1\text{ W m}^{-2} \mu\text{m}^{-1}$  threshold across the entirety of the ASTER observations for day or night separately. The number of  
228 scenes varies per target, but they tend to be between 200-800 observations in total, over the 17 year time period of  
229 satellite observations. However, certain permanent features, such as salt pans, show absorption features in band 11  
230 and therefore have high ratios for the algorithm used. We therefore used a second method that seeks to map transient  
231 absorption features. For this method, we subtract the median from each  $S^t$ , yielding a median deviation stack. By  
232 plotting the maximum deviations across all observations, we then get a map of transient absorption features, in our  
233 case this is mostly volcanic  $\text{SO}_2$  plumes, which map out the cumulative position of different plume observations well.

234 To speed up processing, some of the retrieval runs were binned in order to increase the signal-to-noise ratio, since the  
235 band difference can be rather noisy.

## 236 **2.7 Modelling the anthropogenic CO<sub>2</sub> influence from inventory data**

237 We assessed the likelihood of anthropogenic CO<sub>2</sub>, enhancements of air from San Jose, Costa Rica's capital and main  
238 industrial and population center, influencing our measurements. We used a widely applied Flexible Particle Dispersion  
239 Model (Eckhardt et al., 2017; Stohl et al., 1998, 2005; Stohl and Thomson, 1999) in a forward mode (Stohl et al.,  
240 2005), Flexpart, to simulate the downwind concentrations of CO<sub>2</sub> in the atmosphere (e.g. Belikov et al., 2016), due to  
241 inventory-derived fossil fuel (FF) emissions in our study area for the year 2015 (Fig. 2). The National Centers for  
242 Environmental Prediction (NCEP) - Climate Forecast System Reanalysis (CFSR) 2.5° horizontal resolution  
243 meteorology (Saha et al., 2010b, 2010a), and 1-km Open-Source Data Inventory for Anthropogenic CO<sub>2</sub> (ODIAC;  
244 Oda and Maksyutov, 2011) emissions for 2015 were used to drive the Flexpart model. The CO<sub>2</sub> concentrations were  
245 generated at a 1 km spatial resolution within three vertical levels of the atmosphere (0-100, 100-300, 300-500 meters)  
246 that are possibly relevant to forest canopies in Costa Rica. However, to assess the magnitude of enhancements we only  
247 used CO<sub>2</sub> concentrations observed within the lowest modelled level of the atmosphere, from 0-100 meters. Validation  
248 of the model with direct observations was not required because we were only interested in ensuring that anthropogenic  
249 CO<sub>2</sub> dispersed upslope from San José was not having a significant effect on our study area, we were not aiming to  
250 capture intra-canopy variability, typically at tens to hundreds of ppm variable, which is not relevant to the better  
251 mixed, distal single-digit or less ppm signal from San Jose. The actual concentration of CO<sub>2</sub> and any biogenic influence  
252 in the modelled area was irrelevant because the spatial distribution of anthropogenic CO<sub>2</sub> was the only factor relevant  
253 for this test. 2015 was used as a representative year for simulating the seasonal cycle of CO<sub>2</sub> concentrations that would  
254 be present in any particular year.

## 255 **3 Results**

### 256 **3.1 Volcanic CO<sub>2</sub> emissions through the soil**

257 We measured CO<sub>2</sub> flux emitted through the soil at 66 points over four days (Fig. 1). The first eight points were on  
258 Irazú, and the rest were located near the Ariete fault on Turrialba. We analyzed CO<sub>2</sub> fluxes, not concentrations, because  
259 the diffuse CO<sub>2</sub> emissions through the soil, fed from a deep magma source and dependent on deep permeability, are  
260 highly invariant in time compared to under-canopy air concentrations. In contrast, instantaneous concentration  
261 measurements are modulated by many factors including meteorology, respiration of vegetation and animals, uptake  
262 by plants for photosynthesis, and diurnal dynamic and slope effects. The highly variable concentration measurements  
263 are thus not representative of long-term exposure. The largely invariant soil-to-atmosphere volcanic CO<sub>2</sub> fluxes is  
264 much more representative of long-term exposure, varying mostly spatially and the site-to-site differences are therefore  
265 more representative of the lifetime of exposure of the trees. Mean soil CO<sub>2</sub> flux values over the entire sampling area  
266 varied from 3 to 37 g m<sup>-2</sup> day<sup>-1</sup>, with an average of 11.6 g m<sup>-2</sup> day<sup>-1</sup> and a standard deviation of 6.6 g m<sup>-2</sup> day<sup>-1</sup>. A 12-  
267 bin histogram of mean CO<sub>2</sub> flux shows a bimodal right-skewed distribution with a few distinct outliers (Fig. 3). Fluxes



268 were generally larger on Irazú than on Turrialba. This result agrees with previous studies which showed that the north  
269 flank of Irazú has areas of extremely high degassing, whereas most of our sampling locations on Turrialba were in  
270 areas that had comparatively lower diffuse emissions (Epiard et al., 2017; Stine and Banks, 1991). We used a  
271 cumulative probability plot to identify different populations of CO<sub>2</sub> fluxes (Fig. 3) (Cardellini et al., 2003; Sinclair,  
272 1974).

273 We created an inventory-based model of anthropogenic CO<sub>2</sub> emissions from the San José urban area, parts  
274 of which are less than 15 km from some of our sampling locations (Fig. 2). Our model shows that CO<sub>2</sub> emitted from  
275 San José is blown west to south-west by prevailing winds. Our study area is directly east of San José, and as such is  
276 unaffected by anthropogenic CO<sub>2</sub> from San Jose, which is the only major urban area near Turrialba and Irazú.  
277 Additionally, we used ASTER data to map probabilities of SO<sub>2</sub> across Costa Rica, as a possible confounding factor.  
278 The active craters of both Turrialba and Irazú emit measurable amounts of SO<sub>2</sub>, which is reflected by the high SO<sub>2</sub>  
279 probabilities derived there (Fig. 2). Tropospheric SO<sub>2</sub> quickly converts to sulfate, a well-studied process intensified  
280 by the presence of volcanic mineral ash, plume turbulence, and a humid tropical environment (Oppenheimer et al.,  
281 1989; Eatough et al., 1994); furthermore, the bulk of the SO<sub>2</sub> emissions is carried aloft. Consequently, any remaining  
282 SO<sub>2</sub> causing acid damage effects on trees at Turrialba is limited to a narrow band of a few 100 m around the mostly  
283 quietly steaming central vent, which has been thoroughly ecologically evaluated for acid damage (Jenkins et al., 2012).  
284 D’Arcy (2018) has assessed this narrow, heavily SO<sub>2</sub>-affected area immediately surrounding the central crater vent of  
285 Turrialba, which we avoided, and our sampling sites are mostly within their control zone not considered majorly  
286 affected by SO<sub>2</sub>, but where diffuse CO<sub>2</sub> degassing dominates the excess gas phase (Epiard et al, 2017). Our study area  
287 is on the flanks of the volcano, where ASTER-derived SO<sub>2</sub> probability is minimal, and SO<sub>2</sub> influence not detectable  
288 on the ground (Jenkins et al., 2012; Champion et al., 2012). Most other volcanoes in Costa Rica emit little to no SO<sub>2</sub>  
289 on a decadal time scale, shown by the low or non-existent long-term SO<sub>2</sub> probabilities over the other volcanoes in  
290 Costa Rica (white polygons in Fig. 2).

### 291 **3.2 Tree core isotopes**

292 Bulk wood δ<sup>13</sup>C measurements of all samples in this study, independent of exposure, ranged from -24.03 to -28.12  
293 ‰, with most being clustered around -26 ‰ (Fig. 4). A 5-bin histogram of all δ<sup>13</sup>C measurements shows a slightly  
294 right-skewed unimodal normal distribution, with an average of -26.37 ‰ and a standard deviation of 0.85 ‰. *A.*  
295 *acuminata* and *O. xalapensis* have nearly identical averages (-26.14 and -25.97 ‰, respectively), while *B. nitida* has  
296 a noticeably lighter average of -27.02 ‰. Diffuse excess CO<sub>2</sub> emissions throughout the investigation areas reflect a  
297 deep volcanic source which typically varies little in time (Epiard et al., 2017), but such diffuse emissions spatially  
298 follow geological subsurface structures (Giammanco et al., 1997). Their temporal variability therefore reflects long-  
299 term low-amplitude modulation of the volcanic heavy-δ<sup>13</sup>CO<sub>2</sub> signal, and their spatial distribution is mostly constant  
300 over tree lifetimes, providing a constant long-term spatial gradient of CO<sub>2</sub> exposure to the forest canopy. Our data  
301 show that in areas where CO<sub>2</sub> flux is higher, the wood cores contained progressively higher amounts of <sup>13</sup>C for two of  
302 the three species. Interestingly, our tree core δ<sup>13</sup>C showed no relationship with instantaneous stomatal conductance  
303 for any species, indicating that no stress threshold was exceeded during measurement across the sample set.

### 304 **3.3 Plant function (Fluorescence, Chlorophyll, Stomatal Conductance)**

305 Our measurements and literature data confirm that ecosystems growing in these locations are consistently exposed to  
306 excess volcanic CO<sub>2</sub>, which may impact chlorophyll fluorescence, chlorophyll concentrations, and stomatal  
307 conductance of nearby trees. After excluding visibly damaged trees, leaf fluorescence, expressed as Fv/Fm, was very  
308 high in most samples. Fv/Fm ranged from 0.75 to 0.89, with most measurements clustering between 0.8 and 0.85  
309 (Fig. 5). The fluorescence data has a left-skewed unimodal distribution. The leaf fluorescence (Fv/Fm) values for *A.*  
310 *acuminata* had a strong positive correlation with soil CO<sub>2</sub> flux ( $r^2=0.69$ ,  $p<.05$ ), while the other two species showed  
311 no correlation. No confounding factors measured were correlated with Fv/Fm for any species. In general, *B. nitida*  
312 had the highest Fv/Fm values, and *A. acuminata* and *O. xalapensis* had similar values except for a few *O. xalapensis*  
313 outliers. Chlorophyll concentration measurements were highly variable, ranging from 260 to 922  $\mu\text{mol m}^{-2}$ , with an  
314 average of 558  $\mu\text{mol m}^{-2}$  and a standard deviation of 162  $\mu\text{mol m}^{-2}$  (Fig. 6). Chlorophyll concentration had a  
315 complicated right-skewed bimodal distribution, likely due to the noticeably different averages for each species. *A.*  
316 *acuminata* and *O. xalapensis* both displayed weak correlations between chlorophyll concentration and soil CO<sub>2</sub> flux  
317 ( $r^2=0.38$  and  $r^2=0.28$ , respectively), but their trendlines were found to be almost perpendicular (Fig. 6). As CO<sub>2</sub> flux  
318 increased, *A. acuminata* showed a slight increase in chlorophyll concentration, while *O. xalapensis* had significant  
319 decreases in chlorophyll concentration. *B. nitida* individuals growing on steeper slopes had significantly lower  
320 chlorophyll concentration measurements ( $r^2=0.42$ ,  $p<.05$ ) than those on gentler slopes, a trend not expressed by either  
321 of the other two species ( $r^2=0.01$  for both), demonstrating no significant influence of slope across the majority of  
322 samples. Stomatal conductance ranged from 83.5 to 361  $\text{mmol H}_2\text{O m}^{-2} \text{s}^{-1}$ , with an average of 214  $\text{mmol H}_2\text{O m}^{-2} \text{s}^{-1}$   
323 and a standard deviation of 73.5  $\text{mmol H}_2\text{O m}^{-2} \text{s}^{-1}$ . Distribution was bimodal, with peaks around 150 and 350  
324  $\text{mmol H}_2\text{O m}^{-2} \text{s}^{-1}$ . *A. acuminata* had a moderate positive correlation ( $r^2=0.51$ ) with soil CO<sub>2</sub> flux, but it was not  
325 statistically significant due to a lack of data points (Fig. 7) – however this is a result consistent with the observed  
326 higher chlorophyll concentration (Fig. 6). The other two species displayed no correlation with soil CO<sub>2</sub> flux. *B. nitida*  
327 had a moderate negative correlation ( $r^2=0.61$ ) with slope, similar to its correlation between chlorophyll concentration  
328 and slope.

## 329 **4 Discussion**

### 330 **4.1 Long-term plant uptake of volcanic CO<sub>2</sub>**

331 Turrialba and Irazú continuously emit CO<sub>2</sub> through their vegetated flanks, but prior to this study it was unknown if  
332 the trees growing there were utilizing this additional isotopically heavy volcanic CO<sub>2</sub>. All tree cores with  
333 corresponding CO<sub>2</sub> flux measurements were from areas proximal to the Ariete fault on Turrialba, where atmospheric  
334 and volcanic  $\delta^{13}\text{C}$  have significantly different values (-9.2 and -3.4 ‰, respectively) (Malowany et al., 2017). If the  
335 trees assimilate volcanic CO<sub>2</sub> through their stomata, then we would expect wood  $\delta^{13}\text{C}$  to trend towards heavier values  
336 as diffuse volcanic CO<sub>2</sub> flux increases. After excluding damaged samples and stressed trees,  $\delta^{13}\text{C}$  was strongly  
337 correlated with soil CO<sub>2</sub> flux for both *B. nitida* and *O. xalapensis* (Fig. 4). *A. acuminata* did not have a statistically  
338 significant correlation between soil CO<sub>2</sub> flux and  $\delta^{13}\text{C}$ , likely because it had the fewest data points and a minimal

339 range of CO<sub>2</sub> and δ<sup>13</sup>C values. The difference in regression slope between *B. nitida* and *O. xalapensis* (Fig. 4) may be  
340 due to physiological differences across traits or species, and/or due to differences in exposure owing to canopy height  
341 differences. Resolving this question would require a much larger multi-species sample size which could only be  
342 sufficiently obtained using remote sensing methods. The strong positive correlations between CO<sub>2</sub> flux and  
343 increasingly heavy δ<sup>13</sup>C values suggest that the trees have consistently photosynthesized with isotopically heavy  
344 excess volcanic CO<sub>2</sub> over the last few years, and are therefore growing in eCO<sub>2</sub> conditions. Assuming that all variations  
345 in δ<sup>13</sup>C are caused by the incorporation of heavy volcanic CO<sub>2</sub>, we can calculate the average concentration of the mean  
346 volcanic excess CO<sub>2</sub> in the air the plants are exposed to, with a mass balance equation (Eq. 2):

$$347 \quad C_v = \frac{C_b(\delta_b - \delta_m)}{(\delta_m - \delta_v)} \quad (2)$$

348 where C<sub>v</sub> is the mean volcanic excess component of the CO<sub>2</sub> concentration in air, C<sub>b</sub> is the atmospheric “background”  
349 (i.e., non-volcanic) CO<sub>2</sub> concentration, δ<sub>b</sub> is atmospheric δ<sup>13</sup>C, δ<sub>m</sub> is the difference between background wood δ<sup>13</sup>C  
350 and another wood δ<sup>13</sup>C measurement subtracted from atmospheric δ<sup>13</sup>C, and δ<sub>v</sub> is δ<sup>13</sup>C of the volcanic CO<sub>2</sub>.  
351 Background wood δ<sup>13</sup>C is the value of the point for each species with the lowest CO<sub>2</sub> flux (Fig. 4), and the other wood  
352 δ<sup>13</sup>C measurement is any other point from the same species. Values for δ<sub>v</sub> and δ<sub>b</sub> are taken from Malowany et al. 2017,  
353 and C<sub>b</sub> is assumed to be 400 ppm, a robust invariant since the year-to-year mean northern hemispheric change by ~2  
354 ppm is by far exceeded by local, seasonal, and excess component variability. For the tree core with the highest  
355 measured CO<sub>2</sub> flux for *O. xalapensis*, this equation yields a mean excess volcanic CO<sub>2</sub> concentration of 155 ppm,  
356 bringing the combined mean atmospheric (including volcanic) CO<sub>2</sub> concentration these trees are exposed to, to ~555  
357 ppm. For *B. nitida* this equation yields 190 ppm of mean excess volcanic CO<sub>2</sub> at the highest flux location, for a  
358 combined total mean of ~590 ppm CO<sub>2</sub>. These calculations show that trees in our study area have been consistently  
359 exposed to significantly elevated concentrations of CO<sub>2</sub>, reflective of predicted atmospheric conditions 60-80 years  
360 into the future, assuming a 2 ppm y<sup>-1</sup> mean atmospheric growth rate (Peters et al., 2007), additional measurements of  
361 tree core δ<sup>13</sup>C and associated soil CO<sub>2</sub> fluxes would help corroborate our observations, which were based on a limited  
362 number of data points. Though tree ring <sup>14</sup>C content in volcanically active areas has been linked to variations in  
363 volcanic CO<sub>2</sub> emissions, and comparing patterns of δ<sup>13</sup>C to <sup>14</sup>C measurements for the same wood samples could  
364 provide additional confirmation of this finding (Evans et al., 2010; Lefevre et al., 2017; Lewicki et al., 2014), this  
365 additional dimension was outside the scope of this exploratory study, which focuses on trees’ use of excess <sup>13</sup>C.

366 Our data demonstrate that CO<sub>2</sub> fluxes through the soil are a representative relative measure for eCO<sub>2</sub>  
367 exposure of overlying tree canopies. Forest canopy exposure to volcanic CO<sub>2</sub> will vary over time, as will volcanic  
368 eCO<sub>2</sub>, once emitted through the soil into the sub-canopy atmosphere, the gas experiences highly variable thermal and  
369 wind disturbances which significantly affect dispersion of CO<sub>2</sub> on minute to minute, diurnal, and seasonal timescales  
370 (Staebler and Fitzjarrald, 2004; Thomas, 2011). These processes cause in-canopy measurements of CO<sub>2</sub> concentration  
371 to be highly variable, making instantaneous concentration measurements in a single field campaign not representative  
372 of long-term relative magnitudes of CO<sub>2</sub> exposure. Soil CO<sub>2</sub> fluxes are less tied to atmospheric conditions, and are  
373 primarily externally modulated by rainfall which increases soil moisture and therefore lowers the soil’s gas  
374 permeability (Camarda et al., 2006; Viveiros et al., 2009). These fluxes can also be affected by variations in barometric  
375 pressure, but both of these factors are easily measurable and therefore can be factored in when conducting field work

376 (Viveiros et al., 2009). Assuming the avoidance of significant rainfall and pressure spikes during sampling  
377 (measurements were conducted in the dry season and no heavy rains or significant meteorological variations in  
378 pressure occurred during field work), measuring the input of CO<sub>2</sub> into the sub-canopy atmosphere as soil CO<sub>2</sub> fluxes  
379 is therefore expected to better represent long-term input and exposure of tree canopies to eCO<sub>2</sub> than direct  
380 instantaneous measurements of sub-canopy CO<sub>2</sub> concentration. Previous studies at Turrialba have shown that local  
381 volcanic CO<sub>2</sub> flux is relatively constant on monthly to yearly timescales (de Moor et al., 2016). Therefore, current soil  
382 CO<sub>2</sub> fluxes should give relatively accurate estimates of CO<sub>2</sub> exposure over time. This paper corroborates that  
383 expectation by demonstrating strong correlations between volcanically enhanced soil CO<sub>2</sub> emissions with stable  
384 carbon isotope signals of these emissions documented in the trees' xylem.

385 A study at the previously mentioned Mammoth Mountain tree kill area examined the connection between  
386 δ<sup>13</sup>C and volcanic CO<sub>2</sub> fluxes, but focused on the difference between trees killed by extreme CO<sub>2</sub> conditions and those  
387 that were still alive (Biondi and Fessenden, 1999). They concluded that the changes in δ<sup>13</sup>C that they observed were  
388 due to extreme concentrations of CO<sub>2</sub> (soil CO<sub>2</sub> concentrations of up to 100%) impairing the functioning of root  
389 systems, leading to closure of stomata and water stress (Biondi and Fessenden, 1999). CO<sub>2</sub> does not inherently harm  
390 trees, but the extreme CO<sub>2</sub> concentrations (up to 100% soil CO<sub>2</sub>) at the Mammoth Mountain area caused major soil  
391 acidification, which led to the tree kill (McGee and Gerlach, 1998). We have evidence that those acidification  
392 processes are not affecting our δ<sup>13</sup>C measurements, and that variations in our δ<sup>13</sup>C measurements are more likely to  
393 be caused by direct photosynthetic incorporation of isotopically heavy volcanic CO<sub>2</sub>. Our δ<sup>13</sup>C measurements have no  
394 statistically significant correlation with stomatal conductance, which suggests that our heavier δ<sup>13</sup>C measurements are  
395 not linked to stomatal closure. None of the trees included in the analysis (displayed obvious signs of stress, from water  
396 or other factors, as indicated by their high fluorescence and chlorophyll concentration values and lack of visible  
397 indicators of stress; specifically, our values of Fv/Fm ~0.8 indicate that PSII was operating efficiently in most of the  
398 trees we measured (Baker and Oxborough, 2004). The Mammoth Mountain tree kill areas have several orders of  
399 magnitude higher CO<sub>2</sub> fluxes (well over 10,000 g m<sup>-2</sup> day<sup>-1</sup>) than the areas we sampled (up to 38 g m<sup>-2</sup> day<sup>-1</sup>), making  
400 it much more likely that stress from soil acidification would be causing stomatal closure and affecting wood δ<sup>13</sup>C  
401 measurements at Mammoth Mountain (Biondi and Fessenden, 1999; McGee and Gerlach, 1998; Werner et al., 2014).  
402 In contrast, most of the diffuse degassing at Turrialba does not lead to soil acidification or pore space saturation, as is  
403 evident in our own and others' field data (e.g., Epiard et al 2017). Thus, changes in our δ<sup>13</sup>C values are best explained  
404 by direct photosynthetic incorporation of isotopically heavy volcanic CO<sub>2</sub>. To the best of our knowledge, this is the  
405 first time that a direct correlation between volcanic soil CO<sub>2</sub> flux and wood δ<sup>13</sup>C has been documented. Future studies  
406 should explore this correlation further, as our findings are based on a limited sample size.

#### 407 **4.2 Short-term species response to eCO<sub>2</sub>**

408 Short-term plant functional responses at the leaf level to elevated CO<sub>2</sub> were highly species-dependent. *B. nitida* had  
409 no statistically significant functional responses to soil CO<sub>2</sub> flux and *O. xalapensis* only had a weak negative correlation  
410 between soil CO<sub>2</sub> flux and chlorophyll concentration (Fig. 6.). *A. acuminata*, a nitrogen fixing species, was the only  
411 species with a consistent and positive functional response to elevated CO<sub>2</sub>, displaying a strong positive correlation

412 with fluorescence and a weak positive correlation with chlorophyll concentration and stomatal conductance (Figs. 5-  
413 7). The lack of response in *B. nitida* and *O. xalapensis* could be due to nitrogen limitation, a factor that would not  
414 affect *A. acuminata* due to its nitrogen fixing capability. Previous studies have found that nitrogen availability strongly  
415 controls plant responses to eCO<sub>2</sub> in a variety of ecosystems, including grasslands and temperate forests (Garten et al.,  
416 2011; Hebeisen et al., 1997; Lüscher et al., 2000; Norby et al., 2010). Nitrogen limitation has been posited to be an  
417 important factor in tropical montane cloud forests, and may be contributing to the lack of responses in *B. nitida* and  
418 *O. xalapensis* (Tanner et al., 1998). Due to the exploratory nature of our study, we do not have a large enough dataset  
419 to conclude that the nitrogen fixing capability of species like *A. acuminata* is the cause for its positive response to  
420 volcanically elevated CO<sub>2</sub>, as has been speculated before (Schwandner et al., 2004), but it is a possible correlation that  
421 deserves further investigation. Future studies should explore this correlation further to determine the extent of nitrogen  
422 limitation at Turrialba and Irazú and its impacts on plant responses to eCO<sub>2</sub>.

### 423 **4.3 Lessons Learned for Future Studies**

424 This exploratory study reveals significant new potential for future studies to utilize the volcanically enhanced CO<sub>2</sub>  
425 emissions approach to study tropical ecosystem responses to eCO<sub>2</sub>—one of the largest uncertainties in climate  
426 projections. Costa Rica’s volcanoes are host to large areas of relatively undisturbed rainforest, making them ideal  
427 study areas for examining responses of ecosystems to eCO<sub>2</sub>. However, there are several challenges future studies  
428 should take into consideration if attempting to expand upon this preliminary study. Given the enormous tropical  
429 species diversity and the need to control for confounding factors, large datasets will be needed to answer these  
430 questions conclusively. Field data can be difficult to acquire in these rugged and challenging environments. A remote  
431 sensing approach using airborne measurements, validated by targeted representative ground campaigns, could provide  
432 sufficiently large data sets to represent species diversity and conditions appropriately. Many of the datatypes that  
433 would be useful for this type of study can be acquired from airborne platforms, and remote sensing instruments can  
434 quickly produce the massive datasets required to provide more comprehensive answers to these questions (Cawse-  
435 Nicholson et al., 2018). There are eight forested volcanoes in Costa Rica which are actively degassing CO<sub>2</sub> through  
436 their flanks (Epiard et al., 2017; Liegler, 2016; Melián et al., 2007; de Moor et al., 2016; Williams-Jones, 1997;  
437 Williams-Jones et al., 2000), viable for this type of study (see polygons in Fig. 2). Datasets from those volcanoes  
438 would provide a wider range of altitudes, precipitation levels, temperatures, and other environmental factors that  
439 would help isolate the effects of eCO<sub>2</sub>.

440  
441 Our results also offer significant new tools for the volcanology, where reconstructing past volcano behavior through  
442 eruption histories is hampered by severe preservation gaps in the stratigraphic record. A strong link between  $\delta^{13}\text{C}$  and  
443 volcanic CO<sub>2</sub> could be a game-changer by establishing long-term histories of volcanic CO<sub>2</sub> emission variations. These  
444 proxy signals could be traced back in time using living and preserved dead trees, in order to fill gaps in the historical  
445 and monitoring records – a boon for volcano researchers and observatories to improve eruption prediction capabilities  
446 (Newhall et al., 2017; Pyle, 2017; Sparks et al., 2012). However this would require orders of magnitudes more analyses  
447 than currently done in volcanology. While variations in tree ring <sup>14</sup>C content have been shown to correlate well with

448 variations in volcanic CO<sub>2</sub> flux (Evans et al., 2010; Lefevre et al., 2017; Lewicki and Hilley, 2014), <sup>13</sup>C is inexpensive  
449 to measure at more laboratories, allowing for substantially more data to be acquired. Independent validation, and  
450 calibration by wood core dendrochronology via <sup>14</sup>C, tree rings, or chemical event tracers like sulfur isotopes, could  
451 significantly advance the concept of using wood carbon as archives of past degassing activity. Furthermore, knowledge  
452 of the short-term real-time response of leaves to diffusely emitted eCO<sub>2</sub>, which is more likely to represent deeper  
453 processes inside volcanoes than crater-area degassing (Camarda et al., 2012), may permit the use of trees as sensors  
454 of transient changes in volcanic degassing indicative of volcanic reactivation and deep magma movement possibly  
455 leading up to eruptions (Camarda et al., 2012; Pieri et al., 2016; Schwandner et al., 2017; Shinohara et al., 2008;  
456 Werner et al., 2013).

## 457 **5 Conclusions**

458 We identified multiple areas of dense tropical forest on two Costa Rican active volcanoes that are consistently and  
459 continuously exposed to volcanically-elevated levels of atmospheric CO<sub>2</sub>, diffusively emitted through soils into  
460 overlying forests. These isotopically heavy excess volcanic CO<sub>2</sub> emissions are well correlated with increases in heavy  
461 carbon signatures in wood cores from two species of tropical trees, suggesting long-term incorporation of enhanced  
462 levels of volcanically emitted CO<sub>2</sub> into biomass. Confounding factors that are known to influence δ<sup>13</sup>C values in wood  
463 appear not to have significantly affected our measurements, indicating that the heavier wood δ<sup>13</sup>C values are likely  
464 caused by photosynthetic incorporation of volcanic excess CO<sub>2</sub>. One of the three species studied (*A. acuminata*) has  
465 consistent positive correlations between instantaneous plant function measurements and diffuse CO<sub>2</sub> flux  
466 measurements, indicating that short-term variations in elevated CO<sub>2</sub> emissions may measurably affect trees growing  
467 in areas of diffuse volcanic emissions. These observations reveal significant potential for future studies to use these  
468 areas of naturally elevated CO<sub>2</sub> to study ecosystem responses to elevated CO<sub>2</sub>, and to use trees as sensors of changing  
469 degassing behavior of volcanic flanks, indicative of deep magmatic processes.

470

471 *Data availability.* Data can be found in Table S1 and Table S2 in the supplement or can be requested from Florian  
472 Schwandner (Florian.Schwandner@jpl.nasa.gov).

473

474 *Author contributions.* FMS and JBF designed the study, and RRB, FMS, JBF, and ED conducted the field work and  
475 collected all samples and data with some of the equipment borrowed from GN, who helped interpret the results. TSM  
476 processed the samples for analysis. JPL conducted the SO<sub>2</sub> analysis, wrote the related methods subsection, and helped  
477 interpret the results. VY modelled the anthropogenic CO<sub>2</sub> emissions, wrote the related methods subsection, and helped  
478 interpret the results. CAF created the combined figure showing the CO<sub>2</sub> and SO<sub>2</sub> results and assisted in writing the  
479 manuscript. RRB wrote the publication, with contributions from all co-authors.

480

481 *Competing interests.* The authors declare that they have no conflict of interest.

482 **Acknowledgements**

483 We are grateful for LI-COR, Inc. (Lincoln, NE, USA) providing us a loaner CO<sub>2</sub> sensor for field work in Costa Rica.  
484 We thank Rizalina Schwandner for engineering assistance during sensor integration, OVSICORI (Observatorio  
485 Vulcanológico y Sismológico de Costa Rica, the Costa Rican volcano monitoring authority) for logistical and permit  
486 support, SINAC (Sistema Nacional de Áreas de Conservación, the Costa Rican National Parks Service) for access at  
487 Turrialba volcano, as well as Mr. Marco Antonio Otárola Rojas (Universidad Nacional de Costa Rica – ICOMVIS)  
488 for invaluable help in the field. Incidental funding is acknowledged from the S.W. Hartman Fund at Occidental College  
489 for funding R.R.B.'s field expenses, as well as the Jet Propulsion Laboratory's YIP (Year-round Internship Program)  
490 and the Jet Propulsion Laboratory Education Office for funding and support for R.R.B. F.M.S.'s UCLA contribution  
491 to this work was supported by Jet Propulsion Laboratory subcontract 1570200. Part of the research described in this  
492 paper was carried out at the Jet Propulsion Laboratory, California Institute of Technology, under a contract with the  
493 National Aeronautics and Space Administration.

494 **References**

495 Ainsworth, E. A. and Long, S. P.: What have we learned from 15 years of free-air CO<sub>2</sub> enrichment (FACE)? A meta-  
496 analytic review of the responses of photosynthesis, canopy properties and plant production to rising CO<sub>2</sub>, *New Phytol.*,  
497 165(2), 351–372, doi:10.1111/j.1469-8137.2004.01224.x, 2005.

498 Alvarado, G. E., Carr, M. J., Turrin, B. D., Swisher, C. C., Schmincke, H.-U. and Hudnut, K. W.: Recent volcanic  
499 history of Irazú volcano, Costa Rica: Alternation and mixing of two magma batches, and pervasive mixing, in *Special*  
500 *Paper 412: Volcanic Hazards in Central America*, vol. 412, pp. 259–276, Geological Society of America., 2006.

501 Baker, N. R. and Oxborough, K.: Chlorophyll Fluorescence as a Probe of Photosynthetic Productivity, in *Chlorophyll*  
502 *a Fluorescence*, pp. 65–82, Springer, Dordrecht., 2004.

503 Barquero, R., Lesage, P., Metaxian, J. P., Creusot, A. and Fernández, M.: La crisis sísmica en el volcán Irazú en 1991  
504 (Costa Rica), *Rev. Geológica América Cent.*, 0(18), doi:10.15517/rgac.v0i18.13494, 1995.

505 Belikov, D. A., Maksyutov, S., Yaremchuk, A., Ganshin, A., Kaminski, T., Blessing, S., Sasakawa, M., Gomez-  
506 Pelaez, A. J. and Starchenko, A.: Adjoint of the global Eulerian–Lagrangian coupled atmospheric transport model (A-  
507 GELCA v1.0): development and validation, *Geosci. Model Dev.*, 9(2), 749–764, doi:10.5194/gmd-9-749-2016, 2016.

508 Biondi, F. and Fessenden, J. E.: Response of lodgepole pine growth to CO<sub>2</sub> degassing at Mammoth Mountain,  
509 California, *Ecol. Brooklyn*, 80(7), 2420–2426, 1999.

510 Burton, M. R., Sawyer, G. M. and Granieri, D.: Deep Carbon Emissions from Volcanoes, *Rev. Mineral. Geochem.*,  
511 75(1), 323–354, doi:10.2138/rmg.2013.75.11, 2013.

512 Camarda, M., Gurrieri, S. and Valenza, M.: CO<sub>2</sub> flux measurements in volcanic areas using the dynamic concentration  
513 method: Influence of soil permeability, *J. Geophys. Res. Solid Earth*, 111(B5), B05202, doi:10.1029/2005JB003898,  
514 2006.

515 Camarda, M., De Gregorio, S. and Gurrieri, S.: Magma-ascent processes during 2005–2009 at Mt Etna inferred by  
516 soil CO<sub>2</sub> emissions in peripheral areas of the volcano, *Chem. Geol.*, 330–331, 218–227,  
517 doi:10.1016/j.chemgeo.2012.08.024, 2012.

518 Campion, R., Salerno, G. G., Coheur, P.-F., Hurtmans, D., Clarisse, L., Kazahaya, K., Burton, M., Caltabiano, T.,  
519 Clerbaux, C. and Bernard, A.: Measuring volcanic degassing of SO<sub>2</sub> in the lower troposphere with ASTER band  
520 ratios, *J. Volcanol. Geotherm. Res.*, 194(1–3), 42–54, doi:10.1016/j.jvolgeores.2010.04.010, 2010.

521 Cardellini, C., Chiodini, G. and Frondini, F.: Application of stochastic simulation to CO<sub>2</sub> flux from soil: Mapping and  
522 quantification of gas release, *J. Geophys. Res. Solid Earth*, 108(B9), 2425, doi:10.1029/2002JB002165, 2003.

523 Cawse-Nicholson, K., Fisher, J. B., Famiglietti, C. A., Braverman, A., Schwandner, F. M., Lewicki, J. L., Townsend,  
524 P. A., Schimel, D. S., Pavlick, R., Borman, K., Ferraz, A. A., Ye, Z., Kang, L. E., Ma, P., Bogue, R., Youmans, T.  
525 and Pieri, D. C.: Ecosystem responses to elevated CO<sub>2</sub> using airborne remote sensing at Mammoth Mountain,  
526 California, *Biogeosciences Discuss.*, 2018.

527 Chiodini, G., Cioni, R., Guidi, M., Raco, B. and Marini, L.: Soil CO<sub>2</sub> flux measurements in volcanic and geothermal  
528 areas, *Appl. Geochem.*, 13(5), 543–552, doi:10.1016/S0883-2927(97)00076-0, 1998.

529 Cox, P., Pearson, D., Booth, B., Friedlingstein, P., Huntingford, C., Jones, C. and M Luke, C.: Sensitivity of tropical  
530 carbon to climate change constrained by carbon dioxide variability., 2013.

531 D’Arcy, F.: Novel Methods of volcanic gas measurement using drones and tree ring geochemistry at Turrialba  
532 volcano, Costa Rica. MSc thesis, McGill university, Montreal, Canada, 63 p., 2018. URL:  
533 [http://digitool.Library.McGill.CA:80/R/-?func=dbin-jump-full&object\\_id=154622&silolibrary=GEN01](http://digitool.Library.McGill.CA:80/R/-?func=dbin-jump-full&object_id=154622&silolibrary=GEN01)

534 Dietrich, V. J., Fiebig, J., Chiodini, G. and Schwandner, F. M.: Fluid Geochemistry of the Hydrothermal System, in  
535 Nisyros Volcano, edited by V. J. Dietrich, E. Lagios, and O. Bachmann, p. 339, Springer, Berlin., 2016.

536 Eatough, D.J., Caka, F.M. and Farber, R.J.: The conversion of SO<sub>2</sub> to sulfate in the atmosphere, *Israel J. Chem.*, 34(3-  
537 4), 301-314, 1994.

538 Eckhardt, S., Cassiani, M., Evangeliou, N., Sollum, E., Pisso, I. and Stohl, A.: Source–receptor matrix calculation for  
539 deposited mass with the Lagrangian particle dispersion model FLEXPART v10.2 in backward mode, *Geosci. Model*  
540 *Dev. Katlenburg-Lindau*, 10(12), 4605–4618, doi:http://dx.doi.org/10.5194/gmd-10-4605-2017, 2017.

541 Epiard, M., Avard, G., de Moor, J. M., Martínez Cruz, M., Barrantes Castillo, G. and Bakkar, H.: Relationship between  
542 Diffuse CO<sub>2</sub> Degassing and Volcanic Activity. Case Study of the Poás, Irazú, and Turrialba Volcanoes, Costa Rica,  
543 *Front. Earth Sci.*, 5, doi:10.3389/feart.2017.00071, 2017.

544 Evans, W. C., Bergfeld, D., McGeehin, J. P., King, J. C. and Heasler, H.: Tree-ring 14C links seismic swarm to CO<sub>2</sub>  
545 spike at Yellowstone, USA, *Geology*, 38(12), 1075–1078, 2010.

546 Farrar, C. D., Sorey, M. L., Evans, W. C., Howle, J. F., Kerr, B. D., Kennedy, B. M., King, C.-Y. and Southon, J. R.:  
547 Forest-killing diffuse CO<sub>2</sub> emission at Mammoth Mountain as a sign of magmatic unrest, *Nature*, 376(6542), 675–  
548 678, doi:10.1038/376675a0, 1995.

549 Friedlingstein, P., Meinshausen, M., Arora, V. K., Jones, C. D., Anav, A., Liddicoat, S. K. and Knutti, R.:  
550 Uncertainties in CMIP5 Climate Projections due to Carbon Cycle Feedbacks, *J. Clim.*, 27(2), 511–526,  
551 doi:10.1175/JCLI-D-12-00579.1, 2013.



552 Garten, C. T., Iversen, C. M. and Norby, R. J.: Litterfall 15N abundance indicates declining soil nitrogen availability  
553 in a free-air CO<sub>2</sub> enrichment experiment, *Ecology*, 92(1), 133–139, doi:10.1890/10-0293.1, 2011.

554 Giammanco, S., Gurreri, S. and Valenza, M.: Soil CO<sub>2</sub> degassing along tectonic structures of Mount Etna (Sicily):  
555 the Pernicana fault, *Appl. Geochem.*, 12(4), 429-436, 1997.

556 Global Volcanism Program: Volcanoes of the World, v. 4.6.5, edited by E. Venzke, Smithsonian Inst.,  
557 doi:<https://dx.doi.org/10.5479/si.GVP.VOTW4-2013>, 2013.

558 Gregory, J. M., Jones, C. D., Cadule, P. and Friedlingstein, P.: Quantifying Carbon Cycle Feedbacks, *J. Clim.*, 22(19),  
559 5232–5250, doi:10.1175/2009JCLI2949.1, 2009.

560 Hebeisen, T., Lüscher, A., Zanetti, S., Fischer, B., Hartwig, U., Frehner, M., Hendrey, G., Blum, H. and Nösberger\*,  
561 J.: Growth response of *Trifolium repens* L. and *Lolium perenne* L. as monocultures and bi-species mixture to free air  
562 CO<sub>2</sub> enrichment and management, *Glob. Change Biol.*, 3(2), 149–160, doi:10.1046/j.1365-2486.1997.00073.x, 1997.

563 Jenkins, M.W., Krofcheck, D.J., Teasdale, R., Houppis, J. and Pushnik, J.: Exploring the edge of a natural disaster,  
564 *Open J. Ecol.*, 2(04), 222-232, 2012.

565 Kappelle, M., Geuze, T., Leal, M. E. and Cleef, A. M.: Successional age and forest structure in a Costa Rican upper  
566 montane *Quercus* forest, *J. Trop. Ecol.*, 12(05), 681–698, doi:10.1017/S0266467400009871, 1996.

567 Kauwe, M. G. D., Keenan, T. F., Medlyn, B. E., Prentice, I. C. and Terrer, C.: Satellite based estimates underestimate  
568 the effect of CO<sub>2</sub> fertilization on net primary productivity, *Nat. Clim. Change*, 6(10), 892, doi:10.1038/nclimate3105,  
569 2016.

570 Keeling, C. D.: The Carbon Dioxide Cycle: Reservoir Models to Depict the Exchange of Atmospheric Carbon Dioxide  
571 with the Oceans and Land Plants, in *Chemistry of the Lower Atmosphere*, edited by S. I. Rasool, pp. 251–329, Springer  
572 US, Boston, MA., 1973.

573 Lefevre, J.-C., Gillot, P.-Y., Cardellini, C., Gresse, M., Lesage, L., Chiodini, G. and Oberlin, C.: Use of the  
574 Radiocarbon Activity Deficit in Vegetation as a Sensor of CO<sub>2</sub> Soil Degassing: Example from La Solfatara (Naples,  
575 Southern Italy), *Radiocarbon*, 1–12, doi:10.1017/RDC.2017.76, 2017.

576 Leigh, E. G., Losos, E. C. and Research, N. B. of E.: Tropical forest diversity and dynamism : findings from a large-  
577 scale network, Chicago, Ill.; London: The University of Chicago Press. [online] Available from:  
578 <http://trove.nla.gov.au/version/12851528> (Accessed 25 September 2017), 2004.

579 Lewicki, J. L. and Hilley, G. E.: Multi-scale observations of the variability of magmatic CO<sub>2</sub> emissions, Mammoth  
580 Mountain, CA, USA, *J. Volcanol. Geotherm. Res.*, 284(Supplement C), 1–15, doi:10.1016/j.jvolgeores.2014.07.011,  
581 2014.

582 Lewicki, J. L., Hilley, G. E., Shelly, D. R., King, J. C., McGeehin, J. P., Mangan, M. and Evans, W. C.: Crustal  
583 migration of CO<sub>2</sub>-rich magmatic fluids recorded by tree-ring radiocarbon and seismicity at Mammoth Mountain, CA,  
584 USA, *Earth Planet. Sci. Lett.*, 390, 52–58, doi:10.1016/j.epsl.2013.12.035, 2014.

585 Liegler, A.: Diffuse CO<sub>2</sub> degassing and the origin of volcanic gas variability from Rincon de la Vieja, Miravalles, and  
586 Tenorio volcanoes, Guanacaste province, Costa Rica, Open Access Masters Thesis Mich. Technol. Univ. [online]  
587 Available from: <http://digitalcommons.mtu.edu/etdr/97>, 2016.

588 Lüscher, A., Hartwig, U. A., Suter, D. and Nösberger, J.: Direct evidence that symbiotic N<sub>2</sub> fixation in fertile grassland  
589 is an important trait for a strong response of plants to elevated atmospheric CO<sub>2</sub>, *Glob. Change Biol.*, 6(6), 655–662,  
590 doi:10.1046/j.1365-2486.2000.00345.x, 2000.

591 Malowany, K. S., Stix, J., de Moor, J. M., Chu, K., Lacrampe-Couloume, G. and Sherwood Lollar, B.: Carbon isotope  
592 systematics of Turrialba volcano, Costa Rica, using a portable cavity ring-down spectrometer, *Geochem. Geophys.*  
593 *Geosystems*, 18(7), 2769–2784, doi:10.1002/2017GC006856, 2017.

594 Martini, F., Tassi, F., Vaselli, O., Del Potro, R., Martinez, M., del Laat, R. V. and Fernandez, E.: Geophysical,  
595 geochemical and geodetical signals of reawakening at Turrialba volcano (Costa Rica) after almost 150 years of  
596 quiescence, *J. Volcanol. Geotherm. Res.*, 198(3–4), 416–432, doi:10.1016/j.jvolgeores.2010.09.021, 2010.

597 Mason, E., Edmonds, M. and Turchyn, A. V.: Remobilization of crustal carbon may dominate volcanic arc emissions,  
598 *Science*, 357(6348), 290–294, 2017.

599 McGee, K. A. and Gerlach, T. M.: Annual cycle of magmatic CO<sub>2</sub> in a tree-kill soil at Mammoth Mountain, California:  
600 Implications for soil acidification, *Geology*, 26(5), 463–466, 1998.

601 Melián, G. V., Galindo, I., Pérez, N. M., Hernández, P. A., Fernández, M., Ramírez, C., Mora, R. and Alvarado, G.  
602 E.: Diffuse Emission of Hydrogen from Poás Volcano, Costa Rica, *America Central, Pure Appl. Geophys.*, 164(12),  
603 2465–2487, doi:10.1007/s00024-007-0282-8, 2007.

604 de Moor, J. M., Aiuppa, A., Averd, G., Wehrmann, H., Dunbar, N., Muller, C., Tamburello, G., Giudice, G., Liuzzo,  
605 M., Moretti, R., Conde, V. and Galle, B.: Turmoil at Turrialba Volcano (Costa Rica): Degassing and eruptive processes  
606 inferred from high-frequency gas monitoring, *J. Geophys. Res. Solid Earth*, 121(8), 2016JB013150,  
607 doi:10.1002/2016JB013150, 2016.

608 Newhall, C. G., Costa, F., Ratdomopurbo, A., Venezky, D. Y., Widiwijayanti, C., Win, N. T. Z., Tan, K. and Fajiculay,  
609 E.: WOVOdat – An online, growing library of worldwide volcanic unrest, *J. Volcanol. Geotherm. Res.*, 345, 184–  
610 199, doi:10.1016/j.jvolgeores.2017.08.003, 2017.

611 Norby, R. J., Warren, J. M., Iversen, C. M., Medlyn, B. E. and McMurtrie, R. E.: CO<sub>2</sub> enhancement of forest  
612 productivity constrained by limited nitrogen availability, *Proc. Natl. Acad. Sci.*, 107(45), 19368–19373,  
613 doi:10.1073/pnas.1006463107, 2010.

614 Norby, R. J., De Kauwe, M. G., Domingues, T. F., Duursma, R. A., Ellsworth, D. S., Goll, D. S., Lapola, D. M., Luus,  
615 K. A., MacKenzie, A. R., Medlyn, B. E., Pavlick, R., Rammig, A., Smith, B., Thomas, R., Thonicke, K., Walker, A.  
616 P., Yang, X. and Zaehle, S.: Model–data synthesis for the next generation of forest free-air CO<sub>2</sub> enrichment (FACE)  
617 experiments, *New Phytol.*, 209(1), 17–28, doi:10.1111/nph.13593, 2016.

618 Norman, E. M.: *Buddlejaceae (Flora Neotropica Monograph No. 81)*, The New York Botanical Garden Press., 2000.

619 Oda, T. and Maksyutov, S.: A very high-resolution (1 km×1 km) global fossil fuel CO<sub>2</sub> emission inventory derived  
620 using a point source database and satellite observations of nighttime lights, *Atmos Chem Phys*, 11(2), 543–556,  
621 doi:10.5194/acp-11-543-2011, 2011.

622 Oppenheimer, C., Francis, P. and Stix, J.: Depletion rates of sulfur dioxide in tropospheric volcanic plumes, *Geophys.*  
623 *Res. Lett.*, 25(14), 2671–2674, 1998.

624 Ortega-Pieck, A., López-Barrera, F., Ramírez-Marcial, N. and García-Franco, J.G.: Early seedling establishment of  
625 two tropical montane cloud forest tree species: The role of native and exotic grasses, *For. Ecol. Manage.*, 261(7),  
626 1336-1343, 2011.

627 Paoletti, E., Seufert, G., Della Rocca, G. and Thomsen, H.: Photosynthetic responses to elevated CO<sub>2</sub> and O<sub>3</sub> in  
628 *Quercus ilex* leaves at a natural CO<sub>2</sub> spring, *Environ. Pollut.*, 147(3), 516–524, doi:10.1016/j.envpol.2006.08.039,  
629 2007.

630 Parry, C., Blonquist, J. M. and Bugbee, B.: In situ measurement of leaf chlorophyll concentration: analysis of the  
631 optical/absolute relationship, *Plant Cell Environ.*, 37(11), 2508–2520, doi:10.1111/pce.12324, 2014.

632 Pérez, N., Hernandez, P., Padilla, G., Nolasco, D., Barrancos, J., Melián, G., Padrón, E., Dionis, S., Calvo, D. and  
633 Rodr'iguez, F.: Global CO<sub>2</sub> emission from volcanic lakes., 2011.

634 Peters, W., Jacobson, A. R., Sweeney, C., Andrews, A. E., Conway, T. J., Masarie, K., Miller, J. B., Bruhwiler, L. M.  
635 P., Pétron, G., Hirsch, A. I., Worthy, D. E. J., Werf, G. R. van der, Randerson, J. T., Wennberg, P. O., Krol, M. C. and  
636 Tans, P. P.: An atmospheric perspective on North American carbon dioxide exchange: CarbonTracker, *Proc. Natl.*  
637 *Acad. Sci.*, 104(48), 18925–18930, doi:10.1073/pnas.0708986104, 2007.

638 Pieri, D., Schwandner, F. M., Realmuto, V. J., Lundgren, P. R., Hook, S., Anderson, K., Buongiorno, M. F., Diaz, J.  
639 A., Gillespie, A., Miklius, A., Mothes, P., Mouginiis-Mark, P., Pallister, M., Poland, M., Palgar, L. L., Pata, F.,  
640 Pritchard, M., Self, S., Sigmundsson, F., de Silva, S. and Webley, P.: Enabling a global perspective for deterministic  
641 modeling of volcanic unrest, [online] Available from:  
642 [https://hyspiri.jpl.nasa.gov/downloads/RFI2\\_HyspIRI\\_related\\_160517/RFI2\\_final\\_PieriDavidC-final-rev.pdf](https://hyspiri.jpl.nasa.gov/downloads/RFI2_HyspIRI_related_160517/RFI2_final_PieriDavidC-final-rev.pdf)  
643 (Accessed 20 February 2018), 2016.

644 Pinkard, E. A., Beadle, C. L., Mendham, D. S., Carter, J. and Glen, M.: Determining photosynthetic responses of  
645 forest species to elevated CO<sub>2</sub>: alternatives to FACE, *For. Ecol. Manag.*, 260(8), 1251–1261, 2010.

646 Pyle, D. M.: What Can We Learn from Records of Past Eruptions to Better Prepare for the Future?, in SpringerLink,  
647 pp. 1–18, Springer, Berlin, Heidelberg., 2017.

648 Quintana-Ascencio, P. F., Ramírez-Marcial, N., González-Espinosa, M. and Martínez-Icó, M.: Sapling survival and  
649 growth of coniferous and broad-leaved trees in successional highland habitats in Mexico, *Appl. Veg. Sci.*, 7(1), 81–  
650 88, 2004.

651 Rizzo, A. L., Di Piazza, A., de Moor, J. M., Alvarado, G. E., Avard, G., Carapezza, M. L. and Mora, M. M.: Eruptive  
652 activity at Turrialba volcano (Costa Rica): Inferences from <sup>3</sup>He/ <sup>4</sup>He in fumarole gases and chemistry of the products  
653 ejected during 2014 and 2015: ERUPTIVE ACTIVITY AT TURRIALBA VOLCANO, *Geochem. Geophys.*  
654 *Geosystems*, 17(11), 4478–4494, doi:10.1002/2016GC006525, 2016.

655 Saha, S., Moorthi, S., Pan, H.-L., Wu, X., Wang, J., Nadiga, S., Tripp, P., Kistler, R., Woollen, J., Behringer, D., Liu,  
656 H., Stokes, D., Grumbine, R., Gayno, G., Wang, J., Hou, Y.-T., Chuang, H., Juang, H.-M. H., Sela, J., Iredell, M.,  
657 Treadon, R., Kleist, D., Van Delst, P., Keyser, D., Derber, J., Ek, M., Meng, J., Wei, H., Yang, R., Lord, S., van den  
658 Dool, H., Kumar, A., Wang, W., Long, C., Chelliah, M., Xue, Y., Huang, B., Schemm, J.-K., Ebisuzaki, W., Lin, R.,  
659 Xie, P., Chen, M., Zhou, S., Higgins, W., Zou, C.-Z., Liu, Q., Chen, Y., Han, Y., Cucurull, L., Reynolds, R. W.,

660 Rutledge, G. and Goldberg, M.: NCEP Climate Forecast System Reanalysis (CFSR) 6-hourly Products, January 1979  
661 to December 2010, *Bull. Am. Meteorol. Soc.*, 91(8), 1015–1058, doi:10.5065/D69K487J, 2010a.

662 Saha, S., Moorthi, S., Pan, H.-L., Wu, X., Wang, J., Nadiga, S., Tripp, P., Kistler, R., Woollen, J., Behringer, D., Liu,  
663 H., Stokes, D., Grumbine, R., Gayno, G., Wang, J., Hou, Y.-T., Chuang, H., Juang, H.-M. H., Sela, J., Iredell, M.,  
664 Treadon, R., Kleist, D., Van Delst, P., Keyser, D., Derber, J., Ek, M., Meng, J., Wei, H., Yang, R., Lord, S., van den  
665 Dool, H., Kumar, A., Wang, W., Long, C., Chelliah, M., Xue, Y., Huang, B., Schemm, J.-K., Ebisuzaki, W., Lin, R.,  
666 Xie, P., Chen, M., Zhou, S., Higgins, W., Zou, C.-Z., Liu, Q., Chen, Y., Han, Y., Cucurull, L., Reynolds, R. W.,  
667 Rutledge, G. and Goldberg, M.: The NCEP Climate Forecast System Reanalysis, *Bull. Am. Meteorol. Soc.*, 91(8),  
668 1015–1058, doi:10.1175/2010BAMS3001.1, 2010b.

669 Saurer, M., Cherubini, P., Bonani, G. and Siegwolf, R.: Tracing carbon uptake from a natural CO<sub>2</sub> spring into tree  
670 rings: an isotope approach, *Tree Physiol.*, 23(14), 997–1004, doi:10.1093/treephys/23.14.997, 2003.

671 Schimel, D., Stephens, B. B. and Fisher, J. B.: Effect of increasing CO<sub>2</sub> on the terrestrial carbon cycle, *Proc. Natl.*  
672 *Acad. Sci.*, 112(2), 436–441, doi:10.1073/pnas.1407302112, 2015.

673 Schwandner, F. M., Seward, T. M., Gize, A. P., Hall, P. A. and Dietrich, V. J.: Diffuse emission of organic trace gases  
674 from the flank and crater of a quiescent active volcano (Vulcano, Aeolian Islands, Italy), *J. Geophys. Res.*  
675 *Atmospheres*, 109(D4), D04301, doi:10.1029/2003JD003890, 2004.

676 Schwandner, F. M., Gunson, M. R., Miller, C. E., Carn, S. A., Eldering, A., Krings, T., Verhulst, K. R., Schimel, D.  
677 S., Nguyen, H. M., Crisp, D., O’Dell, C. W., Osterman, G. B., Iraci, L. T. and Podolske, J. R.: Spaceborne detection  
678 of localized carbon dioxide sources, *Science*, 358(6360), eaam5782, doi:10.1126/science.aam5782, 2017.

679 Sharma, S. and Williams, D.: Carbon and oxygen isotope analysis of leaf biomass reveals contrasting photosynthetic  
680 responses to elevated CO<sub>2</sub> near geologic vents in Yellowstone National Park, *Biogeosciences*, 6(1), 25,  
681 doi:10.5194/bg-6-25-2009, 2009.

682 Shinohara, H., Aiuppa, A., Giudice, G., Gurrieri, S. and Liuzzo, M.: Variation of H<sub>2</sub>O/CO<sub>2</sub> and CO<sub>2</sub>/SO<sub>2</sub> ratios of  
683 volcanic gases discharged by continuous degassing of Mount Etna volcano, Italy, *J. Geophys. Res. Solid Earth*,  
684 113(B9), doi:10.1029/2007JB005185, 2008.

685 Sinclair, A. J.: Selection of threshold values in geochemical data using probability graphs, *J. Geochem. Explor.*, 3(2),  
686 129–149, doi:10.1016/0375-6742(74)90030-2, 1974.

687 Sorey, M. L., Evans, W. C., Kennedy, B. M., Farrar, C. D., Hainsworth, L. J. and Hausback, B.: Carbon dioxide and  
688 helium emissions from a reservoir of magmatic gas beneath Mammoth Mountain, California, *J. Geophys. Res. Solid*  
689 *Earth*, 103(B7), 15303–15323, doi:10.1029/98JB01389, 1998.

690 Sparks, R. S. J., Biggs, J. and Neuberg, J. W.: Monitoring Volcanoes, *Science*, 335(6074), 1310–1311,  
691 doi:10.1126/science.1219485, 2012.

692 Staebler, R. M. and Fitzjarrald, D. R.: Observing subcanopy CO<sub>2</sub> advection, *Agric. For. Meteorol.*, 122(3–4), 139–  
693 156, doi:10.1016/j.agrformet.2003.09.011, 2004.

694 Stine, C. M. and Banks, N. G.: Costa Rica Volcano Profile, USGS Numbered Series, U.S. Geological Survey. [online]  
695 Available from: <https://pubs.er.usgs.gov/publication/ofr91591>, 1991.

696 Stohl, A. and Thomson, D. J.: A Density Correction for Lagrangian Particle Dispersion Models, *Bound.-Layer*  
697 *Meteorol.*, 90(1), 155–167, doi:10.1023/A:1001741110696, 1999.

698 Stohl, A., Hittenberger, M. and Wotawa, G.: Validation of the Lagrangian particle dispersion model FLEXPART  
699 against large-scale tracer experiment data, *Atmos. Environ.*, 32(24), 4245–4264, 1998.

700 Stohl, A., Forster, C., Frank, A., Seibert, P. and Wotawa, G.: Technical note: The Lagrangian particle dispersion model  
701 FLEXPART version 6.2, *Atmospheric Chem. Phys.*, 5(9), 2461–2474, doi:https://doi.org/10.5194/acp-5-2461-2005,  
702 2005.

703 Symonds, R. B., Gerlach, T. M. and Reed, M. H.: Magmatic gas scrubbing: implications for volcano monitoring, *J.*  
704 *Volcanol. Geotherm. Res.*, 108(1), 303–341, doi:10.1016/S0377-0273(00)00292-4, 2001.

705 Tanner, E. V. J., Vitousek, P. M. and Cuevas, E.: Experimental Investigation of Nutrient Limitation of Forest Growth  
706 on Wet Tropical Mountains, *Ecology*, 79(1), 10–22, doi:10.1890/0012-9658(1998)079[0010:EIONLO]2.0.CO;2,  
707 1998.

708 Tercek, M. T., Al-Niemi, T. S. and Stout, R. G.: Plants Exposed to High Levels of Carbon Dioxide in Yellowstone  
709 National Park: A Glimpse into the Future?, *Yellowstone Sci.*, 16(1), 12–19, 2008.

710 Thomas, C. K.: Variability of Sub-Canopy Flow, Temperature, and Horizontal Advection in Moderately Complex  
711 Terrain, *Bound.-Layer Meteorol.*, 139(1), 61–81, doi:10.1007/s10546-010-9578-9, 2011.

712 Townsend, A. R., Cleveland, C. C., Houlton, B. Z., Alden, C. B. and White, J. W.: Multi-element regulation of the  
713 tropical forest carbon cycle, *Front. Ecol. Environ.*, 9(1), 9–17, doi:10.1890/100047, 2011.

714 Viveiros, F., Ferreira, T., Silva, C. and Gaspar, J.: Meteorological factors controlling soil gases and indoor CO<sub>2</sub>  
715 concentration: A permanent risk in degassing areas, *Sci. Total Environ.*, 407(4), 1362–1372,  
716 doi:10.1016/j.scitotenv.2008.10.009, 2009.

717 Weng, C., Bush, M. B. and Chepstow-Lusty, A. J.: Holocene changes of Andean alder (*Alnus acuminata*) in highland  
718 Ecuador and Peru, *J. Quat. Sci.*, 19(7), 685–691, doi:10.1002/jqs.882, 2004.

719 Werner, C., Kelly, P. J., Doukas, M., Lopez, T., Pfeffer, M., McGimsey, R. and Neal, C.: Degassing of CO<sub>2</sub>, SO<sub>2</sub>,  
720 and H<sub>2</sub>S associated with the 2009 eruption of Redoubt Volcano, Alaska, *J. Volcanol. Geotherm. Res.*, 259, 270–284,  
721 doi:10.1016/j.jvolgeores.2012.04.012, 2013.

722 Werner, C., Bergfeld, D., Farrar, C. D., Doukas, M. P., Kelly, P. J. and Kern, C.: Decadal-scale variability of diffuse  
723 CO<sub>2</sub> emissions and seismicity revealed from long-term monitoring (1995–2013) at Mammoth Mountain, California,  
724 USA, *J. Volcanol. Geotherm. Res.*, 289, 51–63, doi:10.1016/j.jvolgeores.2014.10.020, 2014.

725 Williams-Jones, G.: The Distribution and Origin of Radon, CO<sub>2</sub> and SO<sub>2</sub> Gases at Arenal Volcano, Costa Rica,  
726 Université de Montréal., 1997.

727 Williams-Jones, G., Stix, J., Heiligmann, M., Charland, A., Lollar, B. S., Arner, N., Garzón, G. V., Barquero, J. and  
728 Fernandez, E.: A model of diffuse degassing at three subduction-related volcanoes, *Bull. Volcanol.*, 62(2), 130–142,  
729 2000.

730

731

732  
733

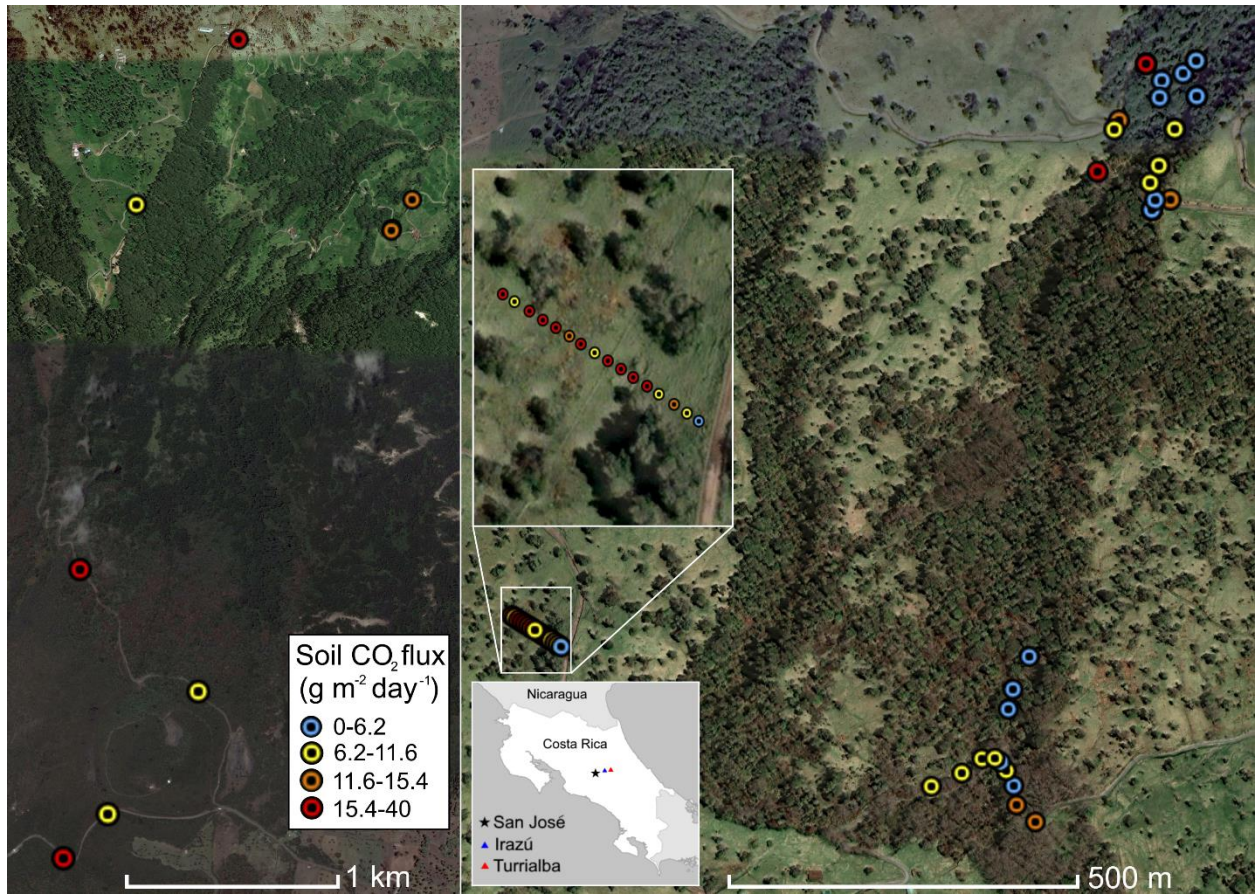
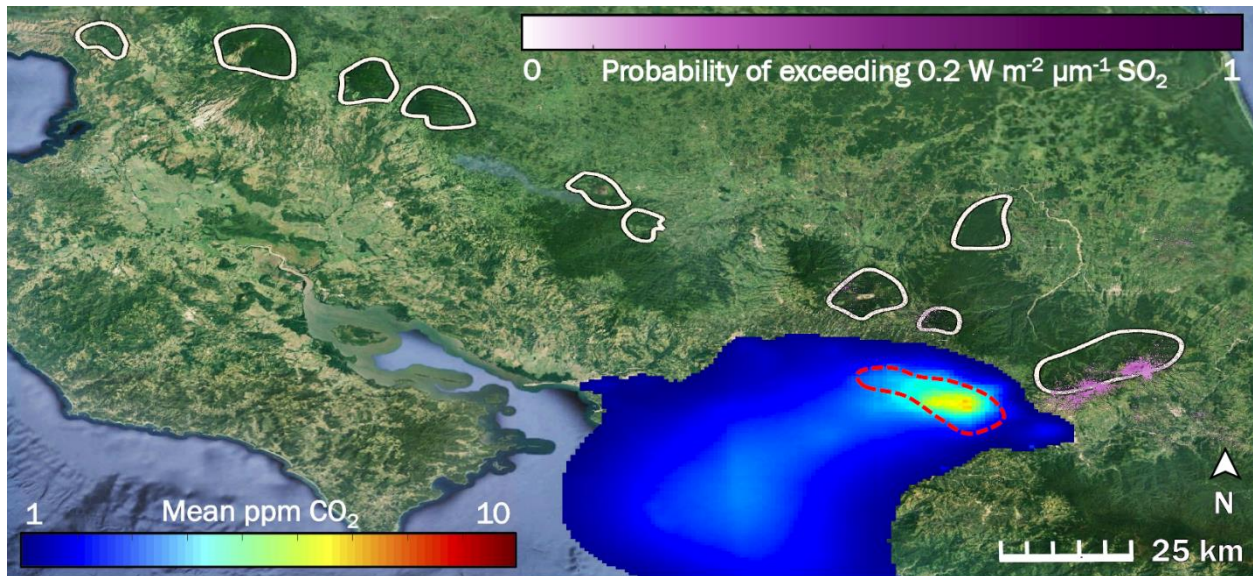


**Fig. 1: Overview of measurement locations in two old-growth forests on the upper flanks of two active volcanoes in Costa Rica, Turrialba and Irazú. Distribution of mean soil CO<sub>2</sub> flux across north flank of Irazú (left) and south flank of Turrialba (right). Colors of dots correspond to flux populations (see Fig. 3).**





734

**Fig. 2:** The influence of two potentially confounding gases on our study area (right hand white polygon) in Costa Rica is low to non-existent: anthropogenic CO<sub>2</sub> from San José (blue to red color scale), and volcanic SO<sub>2</sub> (purple color scale). White polygons are drawn around locations of the forested active volcanic edifices in Costa Rica. The dashed red line indicates the rough border of the San José urban area. Prevailing winds throughout the year consistently blow all anthropogenic CO<sub>2</sub> away from our study area and from all other white polygons.

735  
736  
737

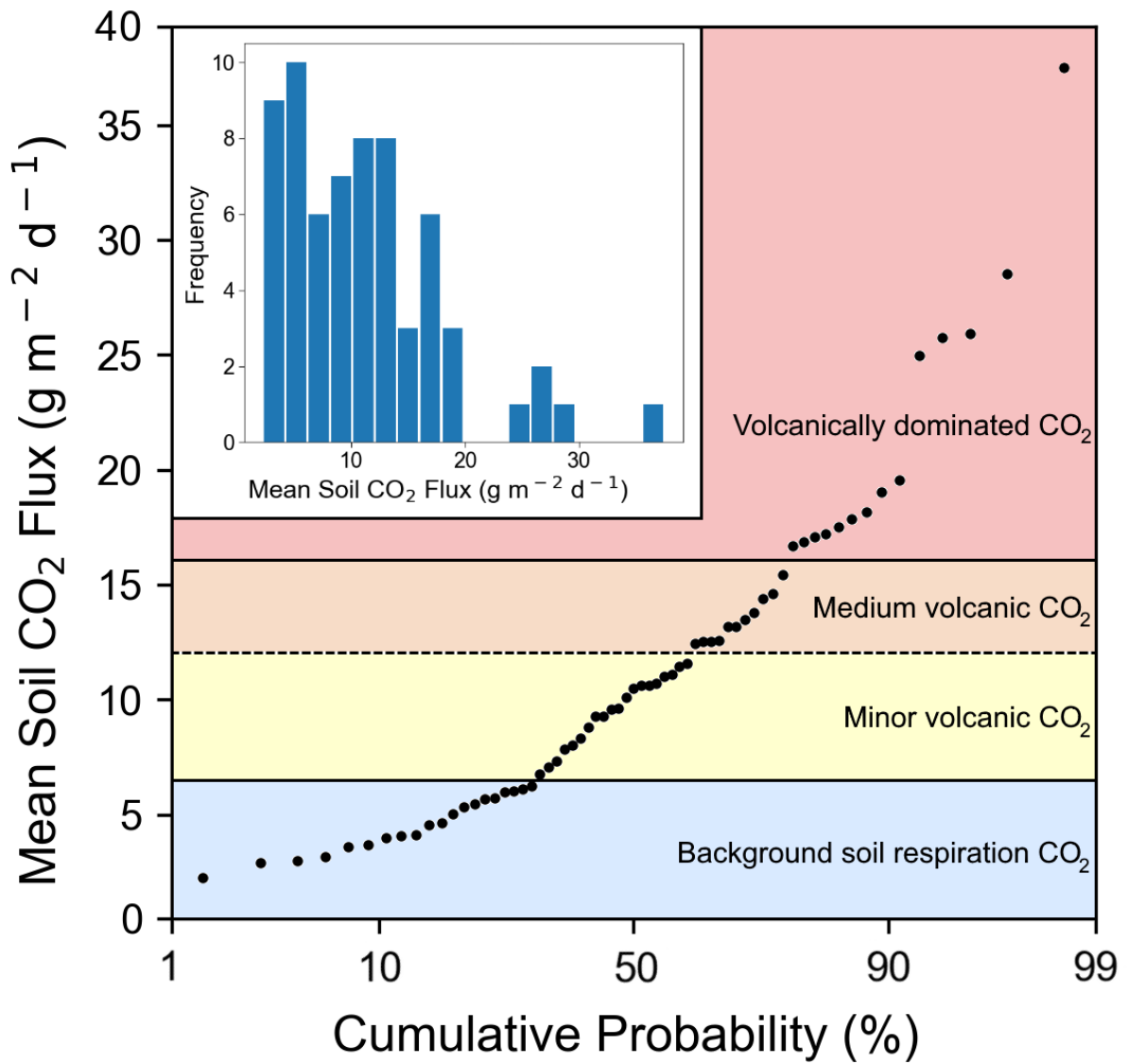


Fig 3: Soil CO<sub>2</sub> flux into the sub-canopy air of forests on the Turrialba-Irazú volcanic complex is pervasively and significantly influenced by a deep volcanic gas source. At least four different overlapping populations of soil CO<sub>2</sub> flux were identified, using a cumulative probability plot, where inflection points indicate population boundaries (Sinclair 1974). 69% of sampling locations (45 total) are exposed to varying degrees of volcanically derived elevated CO<sub>2</sub>. Populations are color-coded based on the same color scale as Fig. 1.



738  
739  
740

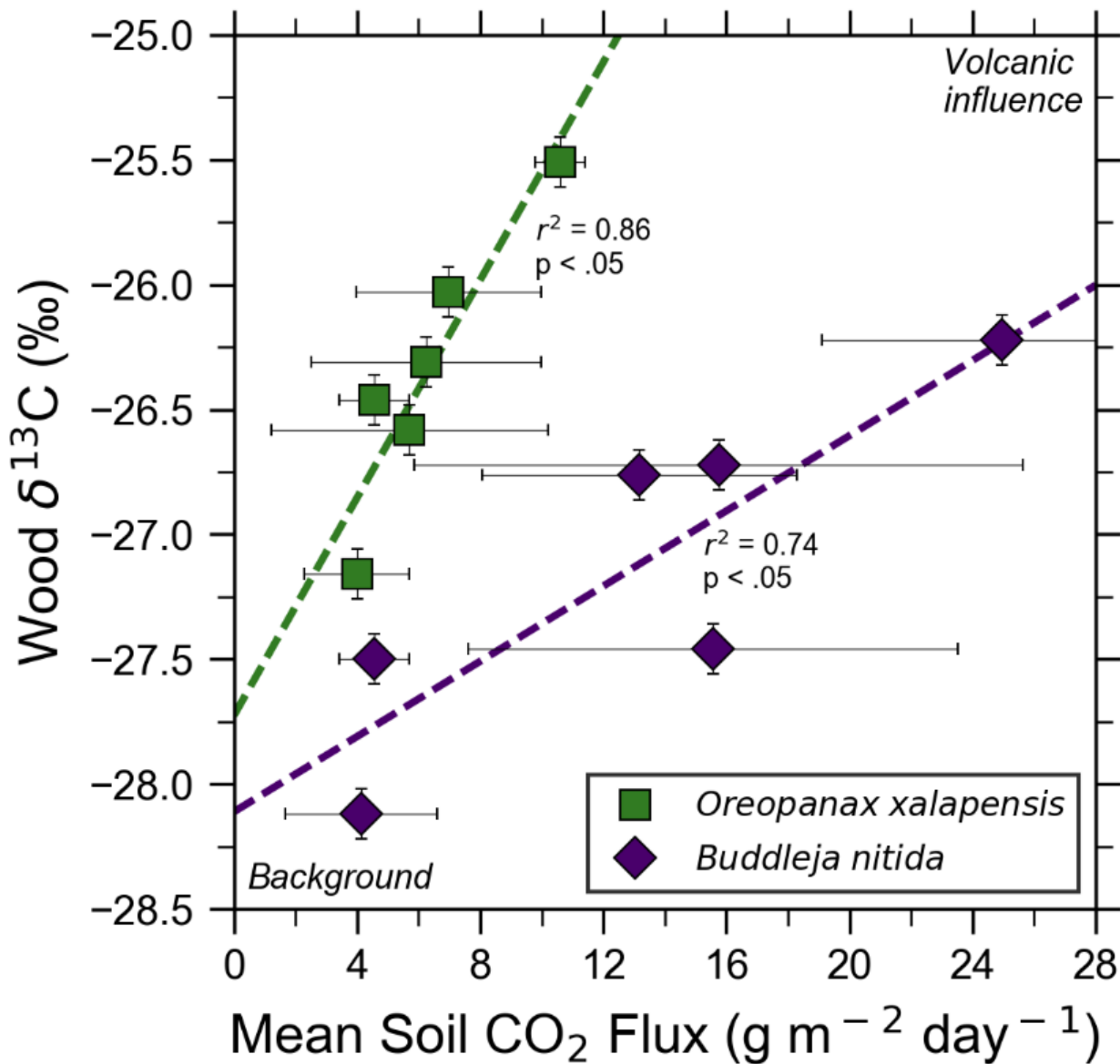


Fig 4: Bulk wood  $\delta^{13}\text{C}$  of trees on Costa Rica's Turrialba volcano shows strong correlations with increasing volcanic  $\text{CO}_2$  flux for two species, *O. xalapensis* and *B. nitida*, indicating long-term photosynthetic incorporation of isotopically heavy volcanic  $\text{CO}_2$ . Stable carbon isotope ratio ( $\delta^{13}\text{C}$ ) of wood cores are plotted against soil  $\text{CO}_2$  flux measured immediately adjacent to the tree that the core sample was taken from. Background and volcanic influence labels apply to both axes – higher  $\text{CO}_2$  flux and heavier (less negative)  $\delta^{13}\text{C}$  values are both characteristic of volcanic  $\text{CO}_2$  emissions.

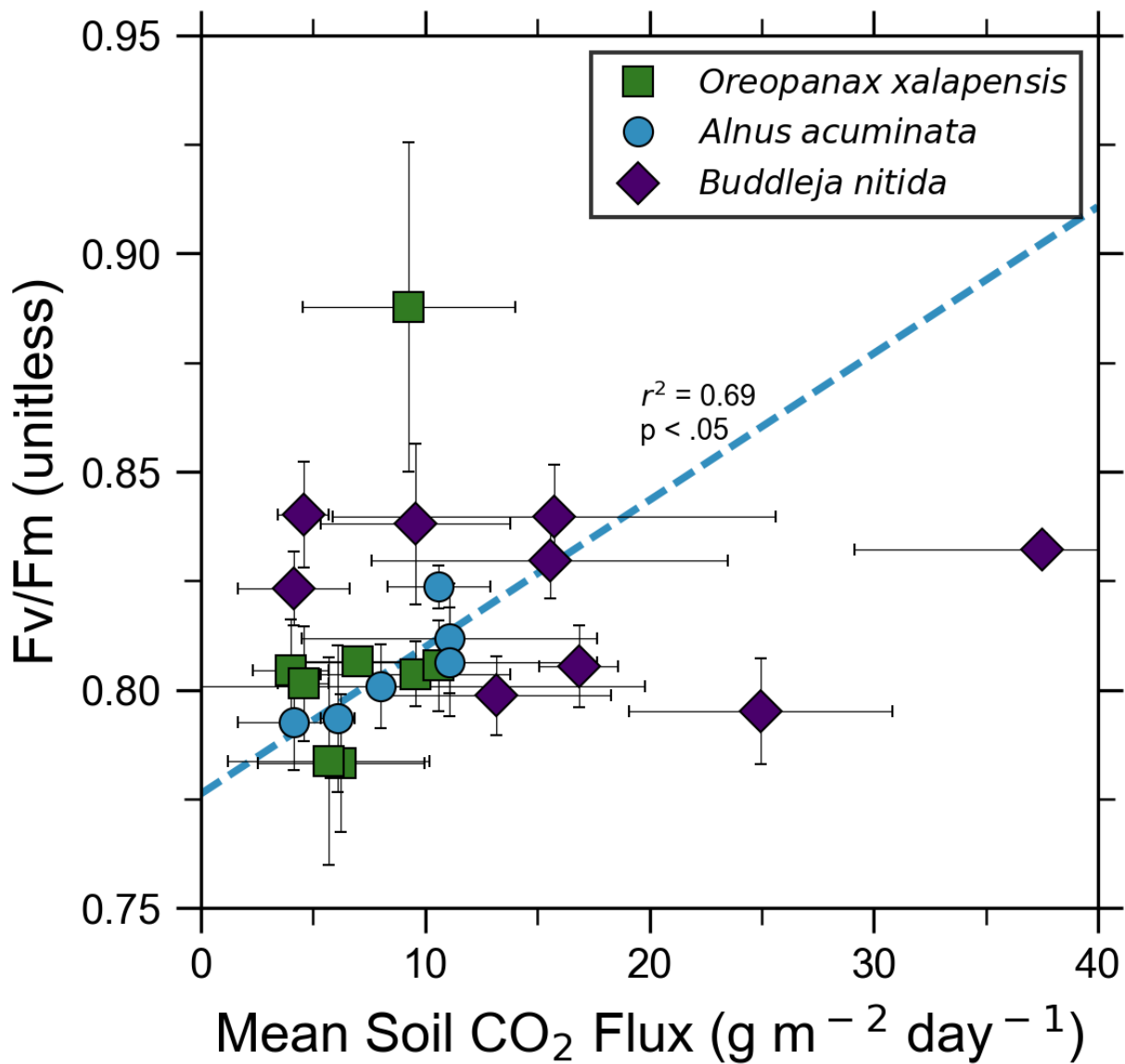
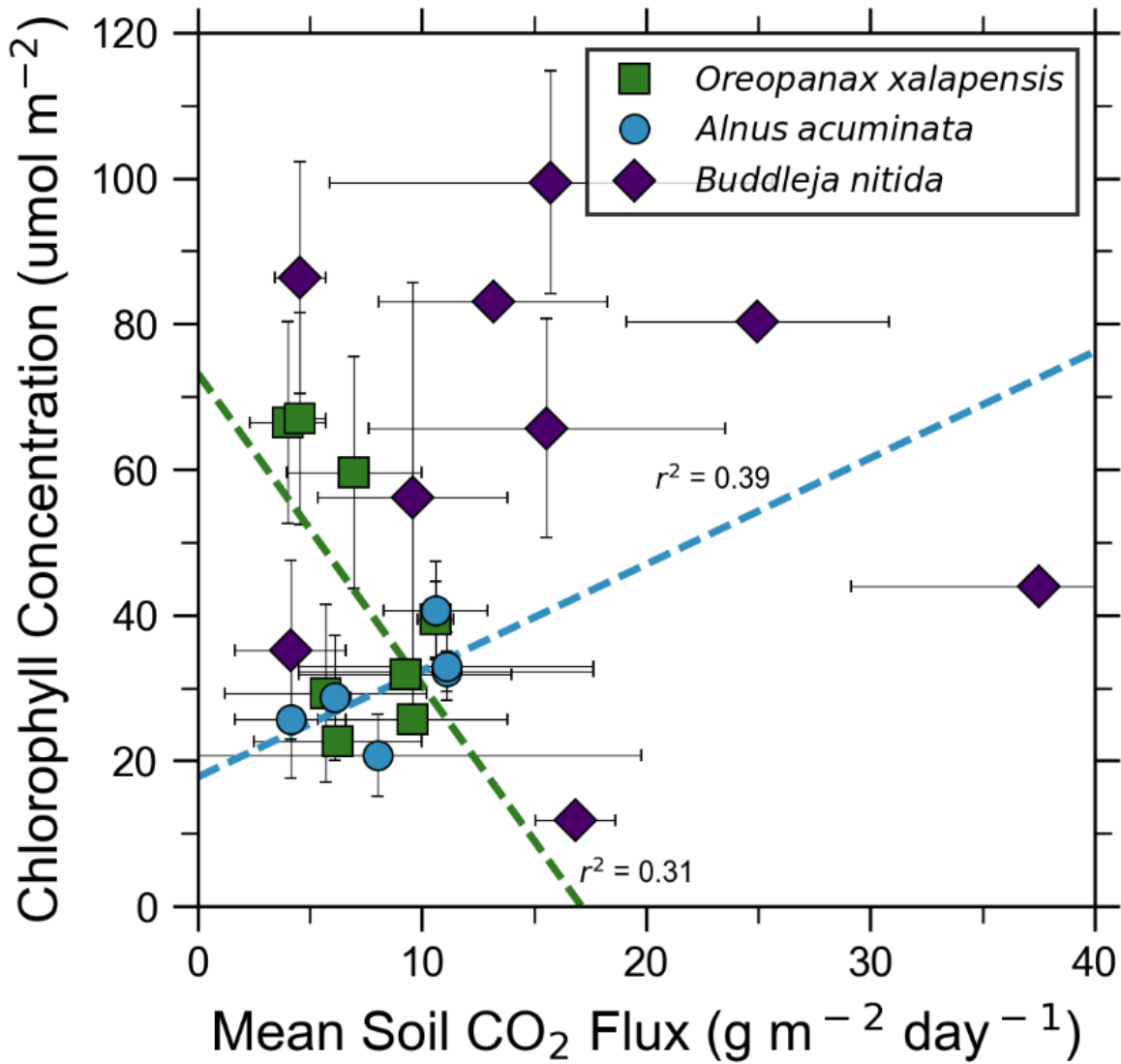


Fig. 5: Photosynthetic activity of some tree species in old-growth forests on the upper flanks of two active volcanoes in Costa Rica, Turrialba and Irazú, may show short-term response to volcanically elevated CO<sub>2</sub>. Leaf fluorescence (Fv/Fm) and soil CO<sub>2</sub> flux were strongly correlated for *A. acuminata*, but not for other species.

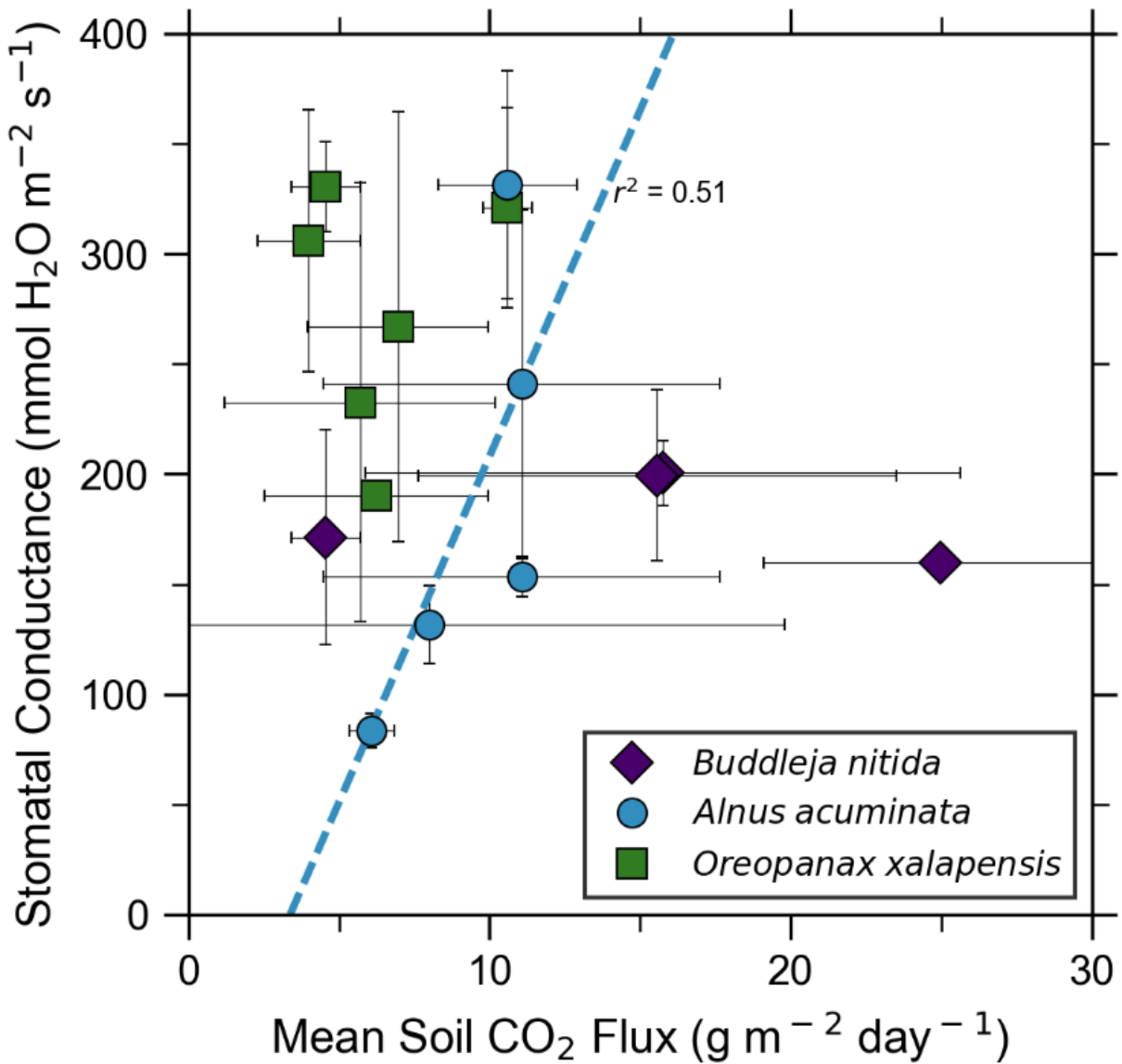


742

Fig. 6: Some tree species in old-growth forests on the upper flanks of two active volcanoes in Costa Rica, Turrialba and Irazú, may express their short-term response to volcanically elevated CO<sub>2</sub> by producing more chlorophyll. A species that showed strong short-term response (*A. Acuminata*, Fig. 5) also shows a positive correlation between chlorophyll concentration and mean soil CO<sub>2</sub> flux.

743

744



745

Fig. 7: Leaf stomatal conductance of a tree species that strongly responds to volcanically elevated CO<sub>2</sub> (Figs. 5, 6) has positive correlations with volcanic CO<sub>2</sub> flux, consistent with increased gas-exchange.

746